Title
A SUCCESSFUL INTEGRAL EQUATION THEORY OF SIMPLE QUANTUM LIQUIDS

Author
Weres, Oleh.

Publication Date
1975

Submitted to Physica

LBL-3234
Preprint c. 1

A SUCCESSFUL INTEGRAL EQUATION THEORY OF SIMPLE QUANTUM LIQUIDS

Oleh Weres

January 1975

Prepared for the U. S. Atomic Energy Commission
under Contract W-7405-ENG-48

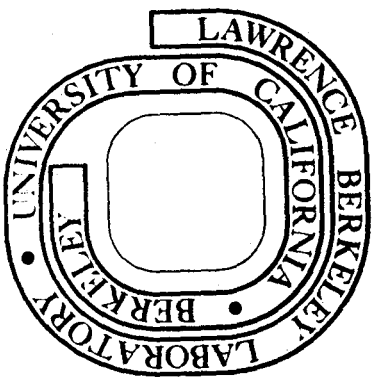

DISCLAIMER

LBL-3234

A SUCCESSFUL INTEGRAL EQUATION THEORY OF SIMPLE QUANTUM LIQUIDS

RUNNING TITLE:

INTEGRAL EQUATIONS FOR QUANTUM LIQUIDS

Oleh Weres*

January 1975

University of California
Lawrence Berkeley Laboratory
Energy and Environment Division
Berkeley, California 94720, USA

---

*The work reported herein was performed while the author was an Adolph C. and Mary Sprague Miller Fellow with the Department of Chemistry of the University of California at Berkeley, and in part by the U.S. Atomic Energy Commission.

ABSTRACT

It is demonstrated that the equilibrium two particle density matrix of a simple quantum liquid may profitably be re-expressed in terms of a Taylor expansion about the diagonal. The resulting arrays of Taylor coefficients are shown to have an intuitive physical significance. A set of three coupled nonlinear integrodifferential equations relating the three most important coefficients is derived.

Approximating certain functions in terms of the straightforwardly calculable dilute gas two particle density matrix Taylor coefficients closes these equations, and they are solved numerically for normal liquid helium -4 and liquid para-hydrogen. Satisfactory results are obtained in both cases. In the case of liquid para-hydrogen a simpler related theory is shown to also yield satisfactory results.

I. INTRODUCTION

The density matrix or statistical operator of an arbitrary N-dimensional system is simply a function of 2N+1 variables when it is written in the Scrödinger representation. These variables are the N-dimensional coordinate vector $\underset{\sim}{x}$, its conjugate vector $\underset{\sim}{x}'$ and the time t. In the equilibrium case, t is replaced by $\beta \equiv (k_B T)^{-1}$. Even when β is effectively disposed of by restricting attention to the equilibrium state at a given temperature, the Schrödinger representation density matrix is a hopelessly unwieldy fundtion if N>1.

In this paper we reduce the equilibrium problem from 2N variables to N variables by replacing $\underset{\sim}{x}$ and $\underset{\sim}{x}'$ by

$$\underset{\sim}{y} \equiv \frac{1}{2}(\underset{\sim}{x}+\underset{\sim}{x}')$$

$$\underset{\sim}{z} \equiv \frac{1}{2}(\underset{\sim}{x}-\underset{\sim}{x}')$$

and Taylor expanding the logarithm of the density matrix in powers of $\underset{\sim}{z}$. We can then dispose of $\underset{\sim}{z}$ by replacing the equilibrium equation for the density matrix by an equaivalent infinite coupled heirarchy of equations relating the non-vanishing even order Taylor coefficients which depend on $\underset{\sim}{y}$ alone.

Specifically, we do this with the equilibrium two particle reduced density matrix of the quantum mechanical Lennard-Jones fluid and the second equation of the quantum mechanical BBGKY heirachy which it must satisfy. The three particle density matrix is eliminated by means of a direct extension of the Kirkwood Superposition Approximation (KSA). The heirarchy is truncated by inserting approximate expressions for the three independent elements of the fourth rank

tensor. These approximate expressions are derived on the basis on the KSA and a simple approximate expression for the off-diagonal structure of the N particle density matrix in terms of the tensors of the dilute gas two particle density matrix which are easily calculable. (The details of this calculation and sample values will be presented elsewhere.) Applying one final approximation and symmetry arguments finally yields a closed set of three scalar integro-differential equations which comprize the quantum mechanical analogue of the Yvon-Born-Green (YBG) equation. In the classical limit, the first of these equations reduces to the classical YBG equation. The equations may be solved numerically for the radial distribution function (rdf) and the two independent elements of the second rank Taylor coefficient tensor.

A simpler theory suggests itself: Why not simply approximate the second rank tensor and solve a single equation for the rdf? Simplifying even further by assuming that the second rank tensor is constant and isotropic yields the Mazo-Kirkwood (MK) theory of simple quantum fluids[1].

We have applied all three of these approaches to both liquid He^4 and liquid p-H_2.* In the case of liquid He^4, the three equation

---

*p-H_2 may safely be considered to be a simple fluid due to its small moment of inertia and the fact that its molecules can only exist in even J states. The small moment of inertia causes the J=0 and J=2 states to be k_Bx525°K apart in energy, thereby effectively restricting all molecules to the rigorously spherically symmetrical J=0 state throughout the temperature range of greatest interest.

approach gives satisfactory results in the normal liquid range, but collapses at the λ-transition line. This is due to the present theory's inability to deal with statistical exchanges which involve more than two particles. The two simpler approaches proved to be totally inadequate for describing liquid helium. These results are presented in Section VII.

In the case of liquid p-H_2, only the Mazo-Kirkwood approach proved unsuitable. Both of the approaches developed in this paper gave satisfactory and nearly identical results. This has the important practical implication that tensors beyond the second rank may be ignored when dealing with any ordinary liquid other than helium. These results are presented in Section VIII.

In both cases the calculated results are quite good at all liquid densities at which the liquids can coexist with their vapors. That is to say, up to the liquid density at the triple point in the case of p-H_2, and up to the λ-transition under own vapor pressure density in the case of He^4. In contrast to this, the classical YBG equation gives rather poor results when it is applied to liquid argon at its triple point density. The reason for this is that the replusive kinetic energy effects in the quantum liquids make them tend to exist at lower densities than do classical liquids. In the proper dimensionless units (which will be defined later) the triple point liquid density of p-H_2 is 0.578, the vapor pressure λ-point liquid density of He^4 is 0.367, and the triple point liquid density of argon is 0.845. All of the approximations which we introduce

become exact in the limit of low density. The low densities at which quantum liquids typically exist render these approximations valid when applied to these substances over the density ranges of greatest interest although they would doubtless collapse if applied at the higher densities which are typical of classical liquids.

A word on our tensor notation: In addition to the usual subscript notation, we use the so-called Gibbsian notation advocated by Drew[2] as it allows us to express our results in a compact form.

All tensors of non-zero rank are in boldface, and the left superscripts indicate the respective ranks. All tensors of rank two or greater will be written with the superscripts throughout. In the case of scalars and vectors, the superscript will be used or not as convenient. In the case of the ${}^{n}\tilde{\tilde{f}}$ tensors, the superscripts also have the significance of function labels.

Binary operators of the sort $\textcircled{2}$ ($\equiv$:) indicate multiple contractions over indices.

$\overset{\gamma}{\nabla}_{\underset{\sim}{x}}$ is the gradient operator, and the subscript indicates which set of variables it operates on.

We write the second rank identity tensor as

$$\delta_{ij} \equiv {}^{2\gamma}\delta = \overset{\gamma\gamma}{ii} + \overset{\gamma\gamma}{jj} + \overset{\gamma\gamma}{kk}$$

Our only notational innovation is the use of the operator Sym $\{\ \}$ which is linear and acts on unit polyads. It replaces a unit polyad by the sum all <u>distinct</u> unit polyads which may be obtained by permuting the argument polyad's indices:

$$\text{Sym}\left\{\underset{ijj}{\sim\sim\sim}\right\} = \underset{ijj}{\sim\sim\sim} + \underset{jij}{\sim\sim\sim} + \underset{jji}{\sim\sim\sim}$$

$$\text{Sym}\left\{\underset{iijj}{\sim\sim\sim\sim}\right\} = \underset{iijj}{\sim\sim\sim\sim} + \underset{ijij}{\sim\sim\sim\sim} + \underset{ijji}{\sim\sim\sim\sim} + \underset{jiij}{\sim\sim\sim\sim} + \underset{jiji}{\sim\sim\sim\sim} + \underset{jjii}{\sim\sim\sim\sim}$$

II. FUNDAMENTAL PROPERTIES OF THE DENSITY MATRIX

The density matrix is a Hermitian operator. Therefore, it undergoes complex conjugation when the sign of $\tilde{z}$ is changed, which is equivalent to interchanging $\tilde{x}$ and $\tilde{x}'$. As the Scrödinger representation of the density matrix is an ordinary complex function, it has a definable logarithm as long as it is nonvanishing. We will concern ourselves with the logarithm only in an infinitesmal neighborhood about the locus $\tilde{x} = \tilde{x}'$. On this locus the non-vanishing value of the density matrix merely requires that the system have a non-vanishing probability of being found in any region of its configurational phase space and that its momentum representation vanish in the limit of infinite momentum. In as far as we have been able to determine, these restrictions are physically meaningless.

Thus we may write

$$\rho(\tilde{x},\tilde{x}';t) = \rho(\tilde{y},\tilde{z};t) \equiv \exp\left[f_o(\tilde{y};t) + i^1\underset{\sim}{f}(\tilde{y};t)\cdot\tilde{z}\right. \qquad (2.1)$$
$$\left. + {}^2\underset{\approx}{f}(\tilde{y};t)\,\textcircled{2}\,\tilde{z}^2 + i^3\underset{\approx\sim}{f}(\tilde{y};t)\,\textcircled{3}\,\tilde{z}^3 + {}^4\underset{\approx\approx}{f}(\tilde{y};t)\,\textcircled{4}\,\tilde{z}^4 + \ldots\right]$$

This form is not altered by going to the classical limit.

In our variables, the definition of the Wigner distribution function[3] (wdf) is written as

$$f_w(\tilde{y},\tilde{p};t) = \left(\frac{1}{\hbar\pi}\right)^N \int d^N\tilde{z}\,\rho(\tilde{y},\tilde{z};t)\,\exp\left(-\frac{2i}{\hbar}\,\tilde{p}\cdot\tilde{z}\right) \qquad (2.2)$$

The wdf is the direct anologue of the classical phase space distribution function. It is perfectly proper to define tensor

moments of the local momentum distribution by

$$\langle p^{\sim n}(\tilde{y};t)\rangle \equiv \frac{\int d^N \tilde{p}\, \tilde{p}^{\sim n} f_w(\tilde{y},\tilde{p};t)}{\int d^N\tilde{p}\, f_w(\tilde{y},\tilde{p};t)}$$

The inverse of (2.2) is

$$\rho(\tilde{y},\tilde{z};t) = \int d^N\tilde{p}\, f_w(\tilde{y},\tilde{p};t)\, \exp\left(\frac{2i}{\hbar}\,\tilde{p}\cdot\tilde{z}\right)$$

Hence,

$$\langle p^n(y;t)\rangle = \frac{\left(\frac{\hbar}{2i}\,\tilde{\nabla}_{\tilde{z}}\right)^n \rho(\tilde{y},\tilde{z};t)\Big|_{\tilde{z}=0}}{\rho(\tilde{y},0;t)}$$

Inserting the form (2.1) into the above, and solving the first four equations of the resulting heirarchy for the first four $^{n}\tilde{\tilde{f}}$ tensors yields

$$^{1}\tilde{f}\,(\tilde{y};t) = \frac{2}{\hbar}\langle\tilde{p}(\tilde{y};t)\rangle$$

$$^{2}\tilde{\tilde{f}}\,(\tilde{y};t) = -\frac{2}{\hbar^2}[\langle\tilde{p}^2(\tilde{y};t)\rangle - \langle p(\tilde{y};t)\rangle^2]$$

$$^{3}\tilde{\tilde{f}}\,(\tilde{y};t) = -\frac{4}{3\hbar^3}[\langle\tilde{p}^3(\tilde{y};t)\rangle - 3\langle\tilde{p}(\tilde{y};t)\rangle\langle\tilde{p}^2(\tilde{y};t)\rangle + 2\langle p(\tilde{y};t)\rangle^3]$$

$$^{4}\tilde{\tilde{f}}\,(\tilde{y};t) = \frac{2}{3\hbar^4}[\langle\tilde{p}^4(\tilde{y};t)\rangle - 4\langle\tilde{p}(\tilde{y};t)\rangle\langle\tilde{p}^3(\tilde{y};t)\rangle - 3\langle\tilde{p}^2(\tilde{y};t)\rangle^2 + 12\langle\tilde{p}^2(\tilde{y};t)\rangle\langle p(\tilde{y};t)\rangle^2 - 6\langle\tilde{p}(\tilde{y};t)\rangle^4]$$

The tensor factors of the right hand sides of these expressions are instantly recognizable as the first four semi-invariants, or cumulants[4], of the local momentum distribution. And thus we arrive at an intuitive physical interpretation of our tensor heirarchy.

In the case that the system has no magnetic forces, the Feynman path integral expression for the equilibrium density matrix shows that it is an everywhere real and non-negative function of $\underset{\sim}{x}, \underset{\sim}{x}'$ and β[5].

This implies the form

$$\rho(\underset{\sim}{y},\underset{\sim}{z};\beta) = \exp[f_o(\underset{\sim}{y};\beta) + {}^{2}\tilde{\tilde{f}}(\underset{\sim}{y};\beta)\,②\,\underset{\sim}{z}^2 + {}^{4}\tilde{\tilde{f}}(\underset{\sim}{y};\beta)\,④\,\underset{\sim}{z}^4 + \ldots] \tag{2.3}$$

for the equilibrium density matrix. In the classical limit this becomes

$$\rho(\underset{\sim}{y},\underset{\sim}{z};\beta) = \exp[-\beta V(\underset{\sim}{y}) - \frac{2}{\hbar^2\beta}\,{}^{2}\tilde{\tilde{M}}\,②\,\underset{\sim}{z}^2]$$

where ${}^{2}\tilde{\tilde{M}}$ is the appropriate mass tensor.

Various relationships between the ${}^{n}\tilde{\tilde{f}}$ tensors may easily be derived. The bulk of this paper is devoted to deriving some of them for the specific case of the two particle reduced density matrix in a liquid. Others will be presented in another publication.

III. LIQUID STATE DENSITY MATRICES

In this section we introduce thedensity matrices appropriate for the description of simple fluids and define the appropriate variables. The one which we shall be most concerned with is the reduced two particle density matrix, which is defined in terms of the N-particle density matrix as

$$\rho_2(\underset{\sim}{R}_1,\underset{\sim}{R}_2,\underset{\sim}{R}_1',\underset{\sim}{R}_2';\beta) = \frac{1}{V^{N-2}}\int d^{3N-6}\underset{\sim}{R}\;\rho_N(\underset{\sim}{R}_N,\underset{\sim}{R}_N';\beta) \tag{3.1}$$

where the integration is over the configuration space of the remaining

N-2 particles. For those particles whose coordinates are integrated over $\tilde{R}_i'$ is set equal to $\tilde{R}_i$ inside the integral. We will also need to deal with the one and three particle density matrices ρ_1 and ρ_3 which are defined analogously. The reduced density matrices have the same general structure as ρ_N and are, of course, real, positive functions. The diagonal values of ρ_2 are proportional to the values of the ordinary radial distribution function (rdf) expressed in the form $g(|\tilde{R}_2-\tilde{R}_1|)$. The constant of proportionality is somewhat arbitrary, and depends on how we choose to normalize our various density matrices. It is most convenient to simply set it equal to unity. This makes the diagonal values of ρ_2 go to unity as $|\tilde{R}_2-\tilde{R}_1| \to \infty$. We further define ρ_1 and ρ_3 to be consistent with this.

We now proceed to define various variables which our arguments shall involve.

$$\tilde{R}_{ij} \equiv \frac{1}{2}(\tilde{R}_i+\tilde{R}_j) \tag{3.2a}$$

$$\tilde{r}_{ij} \equiv \tilde{R}_i-\tilde{R}_j \tag{3.2b}$$

This is simply the transformation to center of mass and relative coordinates for the particles i and j. $\tilde{R}_{ij}'$ and $\tilde{r}_{ij}'$ are defined analogously.

$$\tilde{Y}_i \equiv \frac{1}{2}(\tilde{R}_i+\tilde{R}_i') \tag{3.3a}$$

$$\tilde{Z}_i \equiv \frac{1}{2}(\tilde{R}_i-\tilde{R}_i') \tag{3.3b}$$

$$\tilde{Y}_{ij} \equiv \frac{1}{2}(\tilde{R}_{ij}+\tilde{R}_{ij}') = \frac{1}{2}(\tilde{Y}_i+\tilde{Y}_j) \tag{3.3c}$$

$$\tilde{Z}_{ij} \equiv \frac{1}{2}(\tilde{R}_{ij}-\tilde{R}_{ij}') = \frac{1}{2}(\tilde{Z}_i+\tilde{Z}_j) \tag{3.3d}$$

$$\tilde{y}_{ij} \equiv \frac{1}{2}(\tilde{r}_{ij}+\tilde{r}_{ij}') = \tilde{Y}_i-\tilde{Y}_j \tag{3.3e}$$

$$\tilde{z}_{ij} \equiv \frac{1}{2}(\tilde{r}_{ij}-\tilde{r}_{ij}') = \tilde{Z}_i-\tilde{Z}_j \tag{3.3f}$$

The various $\tilde{y}$'s may properly be considered projections onto the diagonal and the various $\tilde{z}$'s, distances from the diagonal. In cases where the subscripts i and j appear together and are respectively equal to two and one we will, in general, not write them out as a matter of convenience. We will also have need for the following relations:

$$\tilde{r} = \tilde{y}+\tilde{z} \tag{3.4a}$$

$$\tilde{r}' = \tilde{y}-\tilde{z} \tag{3.4b}$$

$$\tilde{Z}_i = \tilde{Z}_{ij}+\frac{1}{2}\tilde{z}_{ij} \tag{3.4c}$$

$$\tilde{Z}_j = \tilde{Z}_{ij}-\frac{1}{2}\tilde{z}_{ij} \tag{3.4d}$$

We will now proceed to determine some further properties of ρ_2. We note that the logarithm of ρ_2 may always be defined in the usual sense. The logarithm must obey the same symmetry requirements as does ρ_2. We are particularly interested in the Taylor coefficients which we obtain by expanding the logarithm of ρ_2 about the diagonal in powers of $\tilde{z}$ and $\tilde{Z}$. These Taylor coefficients are actually the elements of Cartesian tensors, and will be the fundamental objects of our analysis.

The fundamental symmetry condition is that ρ_2 be invariant under the simultaneous interchange $\tilde{R}_1 \rightleftarrows \tilde{R}_1'$ and $\tilde{R}_2 \rightleftarrows \tilde{R}_2'$ since it is an equilibrium density matrix. We shall call this operation I. It is also possible to demonstrate that ρ_2 must be invariant under the

simultaneous interchange $\tilde{R}_1 \rightleftarrows \tilde{R}_2$, $\tilde{R}_1' \rightleftarrows \tilde{R}_2'$. We shall call this operation II. (This symmetry is independent of statistical considerations[6].) Operation I changes the signs of $\tilde{z}$ and $\tilde{Z}$, but leaves $\tilde{y}$ and $\tilde{Y}$ unchanged. This immediately leads us to conclude that only even powers and combinations of $\tilde{z}$ and $\tilde{Z}$ may appear. Therefore, all of the coefficient tensors are of even rank. If we require that the system be homogeneous, all dependence upon the position of the center of mass of particles 1 and 2 must disappear. Since $\tilde{Y}$ is essentially this position, ρ_2 must be independent of $\tilde{Y}$. If we further demand that the system be isotropic, these tensors can depend only on even powers of $\tilde{y}$. (cf. Eqns. (3.6c and e)). Thus the coefficients are not affected by changing the sign of $\tilde{y}$. Operation II changes the signs of $\tilde{y}$ and $\tilde{z}$ but does not effect $\tilde{Y}$ and $\tilde{Z}$. Hence, the only effect of II is to change the sign of $\tilde{z}$, and this means that only even powers of $\tilde{z}$ may appear. We conclude that ρ_2 may rigorously be written in the form

$$\rho_2(\tilde{y},\tilde{z},\tilde{Z};\beta) = \exp[f_o(\tilde{y},\beta) + {}^{2}\tilde{\tilde{f}}(\tilde{y},\beta)\,②\,\tilde{z}^2 + {}^{4}\tilde{\tilde{f}}(\tilde{y};\beta)\,④\,\tilde{z}^4 + {}^{2}\bar{\tilde{f}}(\tilde{y};\beta)\,②\,\tilde{Z}^2 + {}^{4}\bar{\tilde{f}}(\tilde{y};\beta)\,④\,\tilde{z}^2\tilde{Z}^2 + {}^{4}\bar{\bar{\tilde{f}}}(\tilde{y};\beta)\,④\,\tilde{Z}^4 + \ldots] \tag{3.5}$$

As $\tilde{y} \to \infty$, the two particles must decouple if long range forces aren't involved. In this limit the tensors become independent of $\tilde{y}$ and, hence, constant. In particular, as $\tilde{y} \to \infty$, $f_o \to 0$, consistent with our choice of normalization for ρ_2.

The last two tensors vanish in the limit of the dilute gas,

but in general they are non-vanishing. Thus we see that this density matrix is not, in general, factorable into relative and center of mass coordinate dependent portions as it is in the dilute gas limit.

As all of these tensors are arrays of Taylor coefficients, they are invariant under all permutations of indices. The same holds true for the various tensor equations which we shall derive. The fact that they are all (spatial) functions of the three dimensional vector $\tilde{y}$ alone further simplifies matters.

A similar situation is encountered in the case of the various two point tensors dealt with in the theory of homogeneous turbulence. Therefore, the various tensors with which we deal must have the same formal properties as those which arise in the theory of homogeneous turbulence[7] with the additional requirement that they be invariant under all permutations of indices. The most general forms of the tensors of zero through fourth rank which can arise are

$$^{0}T(\tilde{y}) = A(y) \tag{3.6a}$$

$$^{1}T^{i}(\tilde{y}) = y^{i}B(y) \tag{3.6b}$$

$$^{2}T^{ij}(\tilde{y}) = y^{i}y^{j}C(y) + \delta^{ij}D(y) \tag{3.6c}$$

$$^{3}T^{ijk}(\tilde{y}) = y^{i}y^{j}y^{k}E(y) + [y^{i}\delta^{jk}+y^{j}\delta^{ik}+y^{k}\delta^{ij}]F(y) \tag{3.6d}$$

$$\begin{aligned} ^{4}T^{ijkl}(\tilde{y}) &= y^{i}y^{j}y^{k}y^{l}\,G(y) \\ &+ [y^{i}y^{j}\delta^{kl} + y^{i}y^{k}\delta^{jl} + y^{i}y^{l}\delta^{jk} \\ &+ y^{j}y^{k}\delta^{il} + y^{j}y^{l}\delta^{ik} + y^{l}y^{k}\delta^{ij}]H(y) \\ &+ [\delta^{ij}\delta^{kl} + \delta^{ik}\delta^{jl} + \delta^{jk}\delta^{il}]I(y) \end{aligned} \tag{3.6e}$$

where $y = |\tilde{y}|$.

We see that the number of independent components in the various tensors is a simple function of rank: Zeroth and first rank tensors have one each, second and third rank two each, and fourth rank, three.

The general forms presented in (3.6) are fundamental but rather too cumbersome to deal with unless it is absolutely necessary. In particular, the various independent components of the higher rank tensors have different dimensions.

The most expedient alternative appears to be to ignore transformation properties unless absolutely necessary, and simply concentrate on specific elements in some convenient coordinate system. We choose the system in which $\tilde{y} = \hat{\imath} y$. (From now on we will drop most explicit mention of the dependence upon $\tilde{y}$ and β in order to simplify the notation.)

In this system we may write our most important tensors as

$$\tilde{\nabla} V = \hat{\imath} V' \tag{3.7a}$$

$$^2\tilde{\tilde{f}} = k_{\|} \hat{\imath}\hat{\imath} + k_{\perp} (\hat{\jmath}\hat{\jmath} + \hat{k}\hat{k}) \tag{3.7b}$$

$$\tilde{\nabla}^3 V = V''' \, \hat{\imath}\hat{\imath}\hat{\imath} + \left(\frac{V''}{y} - \frac{V'}{y^2}\right) [\mathrm{Sym}\{\hat{\imath}\hat{\jmath}\hat{\jmath}\} + \mathrm{Sym}\{\hat{\imath}\hat{k}\hat{k}\}] \tag{3.7c}$$

$$^4\tilde{\tilde{f}} = h_1 \hat{\imath}\hat{\imath}\hat{\imath}\hat{\imath} + h_2 [\hat{\jmath}\hat{\jmath}\hat{\jmath}\hat{\jmath} + \hat{k}\hat{k}\hat{k}\hat{k} + \tfrac{1}{3} \mathrm{Sym}\{\hat{\jmath}\hat{\jmath}\hat{k}\hat{k}\}]$$
$$+ h_3 [\mathrm{Sym}\{\hat{\imath}\hat{\imath}\hat{\jmath}\hat{\jmath}\} + \mathrm{Sym}\{\hat{\imath}\hat{\imath}\hat{k}\hat{k}\}] \tag{3.7d}$$

All other elements vanish. All other tensors of a given rank must have the same structures. In the following, we will freely

refer to the "$\underset{\sim}{iii}$ element" of one tensor or the "Sym$\{\underset{\sim}{iijj}\}$ elements" of another tensor and generally call them "specific elements".

The independent elements of (3.7) are easily related to those of (3.6). The specific elements of $^2\underset{\approx}{\underset{\sim}{f}}$, $^4\underset{\approx}{f}$ and $^4\underset{\approx}{\underset{\sim}{f}}$ are analogously defined.

In the limit $\underset{\sim}{y} \to \infty$, all of these tensors must be isotropic. Hence, the odd rank tenors vanish identically and

$$k_\perp(\infty) = k_\parallel(\infty)$$

$$h_1(\infty) = h_2(\infty) = 3h_3(\infty)$$

$$^2\underset{\approx}{\underset{\sim}{f}}(\infty) = k_\parallel(\infty)\ ^2\underset{\approx}{\delta} \tag{3.8a}$$

$$^4\underset{\approx}{\underset{\sim}{f}}(\infty) = h_1(\infty)[\underset{\sim}{iiii}+\underset{\sim}{jjjj}+\underset{\sim}{kkkk}+\frac{1}{3}\,\mathrm{Sym}\{\underset{\sim}{iijj}+\underset{\sim}{iikk}+\underset{\sim}{jjkk}\}] \tag{3.8b}$$

The absence of correlation also implies that the two particle density matrix must now factor into the product of two one particle density martrices:

$$\underset{|y| \to \infty}{\mathcal{L}} \rho_2(\underset{\sim}{y},\underset{\sim}{z},\underset{\sim}{Z};\beta) = \rho_1(\underset{\sim}{Z}_1;\beta)\rho_1(\underset{\sim}{Z}_2;\beta)$$
$$\equiv \exp[^2\underset{\approx}{f}_1(\beta)\,②\,(\underset{\sim}{Z}_1^2+\underset{\sim}{Z}_2^2) + {}^4\underset{\approx}{f}_1(\beta)\ ④\ (\underset{\sim}{Z}_1^4+\underset{\sim}{Z}_2^4) + \ldots] \tag{3.9}$$

Eliminating $\underset{\sim}{z}$ and $\underset{\sim}{Z}$ from (3.5) by use of (3.3d and f) and comparing the resulting expression with (3.9) immediately leads us to conclude that in this limit

$$^2\underset{\approx}{\underset{\sim}{f}} = \frac{1}{2}\ ^2\underset{\approx}{\underset{\sim}{f}}_1 \tag{3.10a}$$

$$^2\underset{\approx}{\underset{\sim}{f}} = 4\ ^2\underset{\approx}{\underset{\sim}{f}} = 2\ ^2\underset{\approx}{\underset{\sim}{f}}_1 \tag{3.10b}$$

$$^4\underset{\approx}{\underset{\sim}{f}} = \frac{1}{8}\ ^4\underset{\approx}{\underset{\sim}{f}}_1 \tag{3.10c}$$

$$4\tilde{\tilde{\tilde{f}}} = 24\ {}^{4}\tilde{\tilde{f}} = 3\ {}^{4}\tilde{\tilde{f}}_1 \tag{3.10d}$$

$$4\tilde{\tilde{\tilde{f}}} = 16\ {}^{4}\tilde{\tilde{f}} = 2\ {}^{4}\tilde{\tilde{f}}_1 \tag{3.10e}$$

This shows how the one particle density matrix is contained in the "tail" of the two particle density matrix. ${}^{2}\tilde{\tilde{f}}_1$ and ${}^{4}\tilde{\tilde{f}}_1$ must, of course, have the structures (3.8a and b). This means that each is completely specified by one element.

From (3.10a and b), it is easy to demonstrate that in the limit $\tilde{y} \to \infty$, both the average center of mass kinetic energy of the two particles and their average relative kinetic energy are equal to the average kinetic energy per particle

$$K_1 = K_{rel}(\infty) = -\frac{\hbar^2}{2m}\ {}^{2}\tilde{\tilde{\delta}}(2)\,{}^{2}\tilde{\tilde{f}}(\infty) = -\frac{3}{2}\frac{\hbar^2}{m}\,k_{\|}(\infty) \tag{3.11}$$

IV. THE FUNDAMENTAL EQUATIONS

The equilibrium equation for ρ_2 is[8]

$$H_2\rho_2 - \rho_2 H_2 + n\int d^3\tilde{R}_3[V(\tilde{r}_{31}) + V(\tilde{r}_{32}),\ \rho_3] = 0 \tag{4.1}$$

where

$$n \equiv \frac{N}{V}$$

and

$$\hat{H}_2 = -\frac{\hbar^2}{4m}\nabla^2_{\tilde{R}} - \frac{\hbar^2}{2\mu}\nabla^2_{\tilde{r}} + V(\tilde{r})$$

$$= -\frac{\hbar^2}{16m}\nabla^2_{\tilde{Z}} - \frac{\hbar^2}{8\mu}\left[\nabla^2_{\tilde{y}} + 2\nabla_{\tilde{y}}\cdot\nabla_{\tilde{z}} + \nabla^2_{\tilde{z}}\right] + V(\tilde{y}+\tilde{z})$$

This form operates upon the unprimed coordinates and is appropriate for the first term of (4.1). The form which operates on $\tilde{x}'$ and is appropriate for the second term differs only in the

signs of $\tilde{z}$ and $\tilde{\nabla}_{\tilde{z}}$.

The solution of (4.1) for ρ_2 is contingent upon our being able to find a suitable expression for ρ_3 in terms of ρ_2 and to provide the necessary boundary values.

We choose to eliminate ρ_3 by using the most direct quantum mechanical extension of the KSA

$$\rho_3(1,2,3) \approx \frac{\rho_2(1,2)\rho_2(2,3)\rho_2(1,3)}{\rho_1(1)\rho_1(2)\rho_1(3)} \tag{4.2}$$

which was also employed by Mazo and Kirkwood[1]. We will need ρ_3 only with $\tilde{Z}_3 = 0$, and will concern ourselves only with the scalar and quadratic terms in the logarithm. Simple manipulations convert (4.2) into the form which is most convenient for our purposes:

$$\rho_3 \approx \rho_2(\tilde{y},\tilde{z},\tilde{Z};\beta)\ g\ (\tilde{y}_{31})\ g\ (\tilde{y}_{32})$$

$$\times \exp\{[{}^{2}\tilde{\tilde{f}}^{e}(\tilde{y}_{32}) + {}^{2}\tilde{\tilde{f}}^{e}(\tilde{y}_{31})] \textcircled{2} [\tfrac{1}{4}\tilde{z}^2 + \tilde{Z}^2]$$

$$+ [{}^{2}\tilde{\tilde{f}}^{e}(\tilde{y}_{32}) - {}^{2}\tilde{\tilde{f}}^{e}(\tilde{y}_{31})] \textcircled{2} \tilde{z}\tilde{Z} + \ldots\} \tag{4.3}$$

where

$${}^{2}\tilde{\tilde{f}}^{c}(\tilde{y}) \equiv {}^{2}\tilde{\tilde{f}}^{c}(\tilde{y}) + \frac{1}{4}\,{}^{2}\tilde{\tilde{f}}^{c}(\tilde{y}) \equiv {}^{2}\tilde{\tilde{f}}(\tilde{y}) - {}^{2}\tilde{\tilde{f}}(\infty) + \frac{1}{4}[{}^{2}\tilde{\tilde{f}}(\tilde{y}) - {}^{2}\tilde{\tilde{f}}(\infty)] \tag{4.4}$$

and

$$g = \exp f_o$$

is the ordinary radial distribution function. Of course,

$$\tilde{y}_{31} = \tilde{y}_{32} + \tilde{y}$$

We now insert (3.5) and (4.3) into (4.1), expand the potential terms about $\tilde{z} = 0$, and divide by ρ_2. Many of the integrals which arise from the integrated term in (4.1) vanish due to symmentry. This

gives us an equation in the form of a Taylor expansion, the first three terms of which are proportional to $\underset{\sim}{z}$, $\underset{\sim}{z}^3$, and $\underset{\sim}{z}\underset{\sim}{Z}^2$. These three coefficients are our fundamental equations in tensor form. Before writing them out, we introduce a simplifying change of variables

$$\underset{\sim}{\omega} \equiv -\underset{\sim}{y}_{32}$$

$$-(\underset{\sim}{\omega}-\underset{\sim}{y}) = \underset{\sim}{y}_{31}$$

and note that

$$\underset{\sim}{\nabla}_{\underset{\sim}{\omega}} = -\underset{\sim}{\nabla}_{\underset{\sim}{y}_{32}}$$

$$\underset{\sim}{\nabla}_{\underset{\sim}{\omega}-\underset{\sim}{y}} = -\underset{\sim}{\nabla}_{\underset{\sim}{y}_{31}}$$

$$\int d^3\underset{\sim}{\omega} = \int d^3\underset{\sim}{y}_{32}$$

The coefficient of $\underset{\sim}{z}$ is proportional to

$$-\frac{\hbar^2}{2\mu}\left[\underset{\sim}{\nabla}\cdot{}^2\underset{\approx}{f} + {}^2\underset{\approx}{f}\cdot\underset{\sim}{\nabla}f_o\right]+\underset{\sim}{\nabla}V+n\int g(|\underset{\sim}{\omega}|)g(|\underset{\sim}{\omega}-\underset{\sim}{y}|)\underset{\sim}{\nabla}_{\underset{\sim}{\omega}}V(\underset{\sim}{\omega})d^3\underset{\sim}{\omega} = 0 \quad (4.5a)$$

the coefficient of $\underset{\sim}{z}^3$ is proportional to

$$-\frac{\hbar^2}{2\mu}\left[2\underset{\sim}{\nabla}\cdot{}^4\underset{\approx}{f}+2\ {}^4\underset{\approx}{f}\cdot\underset{\sim}{\nabla}f_o + {}^2\underset{\approx}{f}\cdot\underset{\sim}{\nabla}({}^2\underset{\approx}{f})\right]+\frac{1}{6}\underset{\sim}{\nabla}^3V$$

$$+\frac{n}{24}\int g(|\underset{\sim}{\omega}|)g(|\underset{\sim}{\omega}-\underset{\sim}{y}|)\{\underset{\sim}{\nabla}^3_{\underset{\sim}{\omega}}V(\underset{\sim}{\omega}) + 6^2\underset{\approx}{f}^e(\underset{\sim}{\omega})[\underset{\sim}{\nabla}_{\underset{\sim}{\omega}}V(\underset{\sim}{\omega})-\underset{\sim}{\nabla}_{\underset{\sim}{\omega}-\underset{\sim}{y}}V(\underset{\sim}{\omega}-\underset{\sim}{y})]\}d^3\underset{\sim}{\omega} = 0 \quad (4.5b)$$

the coefficient of $\underset{\sim}{z}\underset{\sim}{Z}^2$ is proportional to

$$-\frac{\hbar^2}{2\mu}\left[\underset{\sim}{\nabla}\cdot{}^4\underset{\approx}{\overline{f}} + {}^4\underset{\approx}{\overline{f}}\cdot\underset{\sim}{\nabla}f_o + {}^2\underset{\approx}{\overline{f}}\cdot\underset{\sim}{\nabla}({}^2\underset{\approx}{\overline{f}})\right]$$

$$+\frac{n}{2}\int g(|\underset{\sim}{\omega}|)g(|\underset{\sim}{\omega}-\underset{\sim}{y}|)\{\underset{\sim}{\nabla}^3_{\underset{\sim}{\omega}}V(\underset{\sim}{\omega}) + {}^2\underset{\approx}{f}^e(\underset{\sim}{\omega})[2\underset{\sim}{\nabla}_{\underset{\sim}{\omega}-\underset{\sim}{y}}V(\underset{\sim}{\omega}-\underset{\sim}{y})+6\underset{\sim}{\nabla}_{\underset{\sim}{\omega}}V(\underset{\sim}{\omega})]\}d^3\underset{\sim}{\omega} = 0 \quad (4.5c)$$

(Unlabeled functions and gradients depend on $\tilde{y}$.)

All other coefficients of up to and including the third rank vanish. (4.5a) is a vector equation and the other two, third rank tensor equations. f_o, $^2\tilde{\tilde{f}}$ and $^2\tilde{\tilde{\tilde{f}}}$ together have a total of five independent elements; i.e., they are completely determined by five scalar functions which depend only on y and β. $^4\tilde{\tilde{f}}$ and $^4\tilde{\tilde{\tilde{f}}}$ have a total of six independent elements. $^4\tilde{\tilde{\tilde{\tilde{f}}}}$ does not appear and $^2\tilde{\tilde{f}}^e$ is determined by $^2\tilde{\tilde{f}}$ and $^2\tilde{\tilde{\tilde{f}}}$ (cf. (4.4)). We see that Eqns. (4.5) are equivalent to five scalar equations in eleven unknowns. In Section VI we will derive approximate expressions for the fourth rank tensors. Inserting these expressions into Eqns. (4.5) results in a closed set of five scalar equations in five scalar unknowns.

Since these equations are of the coupled non-linear integro-differential variety, it seems desireable to attempt to reduce the number. We note that in the limit $n \to 0$ (4.5c) degenerates into $0 = 0$ leaving (4.5a and b) as the fundamental equations for the dilute gas two particle density matrix. Since quantum liquids have rather low densities, we conclude that somehow disposing of (4.5c) is the simplification of choice. This view is strengthened by the observation that (4.5a and b) are coupled to (4.5c) only through the appearance of $^2\tilde{\tilde{f}}^e$ (which contains $^2\tilde{\tilde{\tilde{f}}}^c$ or, equivalently $^2\tilde{\tilde{\tilde{f}}}$) in (4.5b). The limited nature of this coupling suggests that introducing an approximation for $^2\tilde{\tilde{\tilde{f}}}^c$ into (4.5b) might be reasonably safe.

In Section VI we shall see that a reasonable approximation is

$$2\tilde{\tilde{f}}^{c} = 4(2\tilde{\tilde{f}}^{c} - 2\tilde{\tilde{f}}^{d}) \tag{4.6}$$

where $2\tilde{\tilde{f}}^{d}$ is the $2\tilde{\tilde{f}}^{c}$ of the dilute gas two particle density matrix at the given temperature. As we noted in the introduction, the elements of $2\tilde{\tilde{f}}^{d}$ are easy to calculate and may, therefore, be considered to be given functions. This gives us

$$2\tilde{\tilde{f}}^{e} \approx 2^{2}\tilde{\tilde{f}}^{c} - 2\tilde{\tilde{f}}^{d} \tag{4.7}$$

and, given that we can obtain a suitable approximate expression for $4\tilde{\tilde{f}}$ and provide the boundary value $2\tilde{\tilde{f}}(\infty)$, (4.5a and b) become equivalent to a closed set of three scalar equations in three scalar unknowns. (We will not concern ouselves with (4.5c) any further.)

If a suitable approximation is available for $2\tilde{\tilde{f}}$, we may further simplify matters by solving (4.5a) alone for f_o or, equivalently g. (4.5a) is the fundamental equation with which Mazo and Kirkwood[1] began. The use of (4.5a) alone is the most direct extension of the classical YBG theory.

Using (3.11) and the fact that in the classical limit $K_{rel} = \frac{3}{2} k_B T$ and is independent of y we see that in this limit

$$2\tilde{\tilde{f}} = -\frac{2\mu}{\hbar^2\beta} 2\tilde{\tilde{\delta}} = -\frac{2\mu k_B T}{\hbar^2} 2\tilde{\tilde{\delta}}$$

Substituting this into (4.5a) quickly leads us to the classical YBG equation:

$$\tilde{\nabla} \log g + \beta\tilde{\nabla}V + n\beta\int g(|\tilde{\omega}|)g(|\tilde{\omega}-\tilde{y}|)\tilde{\nabla}_{\tilde{\omega}}V(\tilde{\omega})d^{3}\tilde{\omega} = 0 \tag{4.8}$$

The way in which Mazo and Kirkwood actually applied (4.5a) is summed up by the approximation

$$2\tilde{\tilde{f}} \approx -\frac{2\mu k_B T_{eff}}{\hbar^2} 2\tilde{\tilde{\delta}}$$

which, upon being inserted into (4.5a), yields an equation identical to (4.8) except for the substitution of $(k_B T_{eff})^{-1}$ for β. We shall refer to T_{eff} as "the effective temperature". Mazo and Kirkwood did not propose any ab initio method for evaluating it.

In closing this section, we note that attempting to derive (4.5b) by analogy to the usual "mean field force" derivation of (4.8) would result in the numerical coefficient of the $\hat{\nabla}^3 V$ dependent integrated term being four times greater than it actually is. This "mean field dimunition effect" is due to the various coordinate transforms which enter into the correct derivation which we have actually employed. It gives us reason to hope that the additional error introduced by employing the extended KSA (4.1) in (4.5b) is of limited magnitude.

V. REDUCTION TO SCALAR EQUATIONS AND DIMENSIONLESS VARIABLES

We will employ the usual Lennard-Jones potential function

$$V(y) = 4\epsilon\left[\left(\frac{\sigma}{y}\right)^{12} - \left(\frac{\sigma}{y}\right)^{6}\right]$$

where σ is the so-called collision diameter and ϵ is the depth of the potential well. We will use them as our fundamental units of length and energy and the reduced mass $\mu = \frac{m}{2}$ as our fundamental unit of mass. Quantities expressed in these units will be referred to as "reduced" or "dimensionless."

In our final result, all of these parameters, along with $\hbar$ will be lumped together into powers of the DeBoer parameter

$$\Lambda \equiv \frac{\hbar}{\sigma\sqrt{2\mu\epsilon}}$$

which is the dimensionless equivalent of $\hbar$. We present the values of these various parameters for He^4 and p-H_2 in Table 1.

The reduced equivalents of β and the number density n are

$$t \equiv \varepsilon\beta$$

$$\rho \equiv n\sigma^3$$

With few exceptions we will retain the same symbols for the various functions and variables in order to simplify the transition. The main exception is in regard to $^2\tilde{\tilde{f}}$. With $\tilde{y} = \tilde{i}y$ this tensor has the structure (3.7b). We replace $k_{\|}$ and $k_{\perp}$ by

$$K_{\|}(y) \equiv -\frac{\hbar^2}{4\mu\varepsilon} k_{\|}(y)$$

$$K_{\perp}(y) \equiv -\frac{\hbar^2}{4\mu\varepsilon} k_{\perp}(y)$$

which are energies expressed in the unit ε. The classical limit values are equal to $\frac{1}{2t}$. We don't do this with the elements of $^2\tilde{\tilde{f}}^e$, but rather express them in units of σ^{-2} and retain the same symbol. From this point on we will concern ourselves with reduced quantities with no further comment.

Now we proceed to sketch the reduction of Eqns. (4.5a and b) to scalar form. We set $\tilde{y} = \tilde{i}y$. The scalar equations which we will derive are simply the three distinct elements which appear in (4.5a and b) when we fix $\tilde{y}$ in this way (i.e., the "specific elements" of (4.5a and b)). (4.5a) is clearly a vector equation whose terms are all parallel to $\tilde{y}$ and, therefore, we need concern ourselves only with the $\tilde{i}$ component of each term. (4.5b) has two distinct specific

elements: The $\overset{\sim\sim\sim}{iii}$ element, and the element common to all of the unit polyads in Sym$\{\overset{\sim\sim\sim}{ijj}+\overset{\sim\sim\sim}{ikk}\}$. At some points in these manipulations non-equal expressions for these six elements may arise. Occasionally this is caused by a notational inconsistency to which both Gibbsian and "subscript" notation are prone. This problem is correctly disposed of by averaging the six elements after all tensor manipulations are completed. This situation also arises from the fact that the integrand in (4.5b) is a tensor. We know that the proper structure must result when we perform the integration. However, it proves more convenient to force the symmetry on the integrand before performing the integration, as this greatly reduces the number and complexity of the integrals which must be dealt with. In particular, it reduces the integrals from three dimensions to two. We replace the integration variable $\tilde{\omega}$ by the equivalent set of spherical coordinates defined by

$$\omega_x = \omega \cos \theta$$

$$\omega_y = \omega \sin \phi \sin \theta$$

$$\omega_z = \omega \cos \phi \sin \theta$$

with the substitution

$$\mu \equiv \cos \theta$$

$$\int_0^{\pi} \sin \theta d\theta = \int_{-1}^{1} d\mu$$

(We beg the reader's pardon for the double meaning assigned to the symbol μ. Both meanings are established usage and should cause no confusion as they never occur together).

The scalar equivalent of (4.5a) is

$$K_{\|}^{|} + \frac{2}{y}(K_{\|}-K_{\perp}) + f^{|}K_{\|} + \frac{1}{2}V^{|} \qquad (5.1)$$

$$+ \pi\rho\int_0^{\infty}\omega^2 d\omega\int_{-1}^{1}\mu d\mu g(\omega)V^{|}(\omega)g(\sqrt{\omega^2+y^2-2y\omega\mu}) = 0$$

The $\tilde{i}\tilde{i}\tilde{i}$ element of (4.5b) is

$$\frac{\Lambda^4}{2}[G_1+f^{|}h_1]+K_{\|}K_{\|}^{|} - \frac{\Lambda^2}{24}V^{\|\|} - \frac{\Lambda^2}{8}\pi\rho\int_0^{\infty}\omega^2 d\omega\int_{-1}^{1}d\mu g(\omega)g(|\tilde{\omega}-\tilde{y}|)$$

$$X[D(\omega)\mu^3+C(\omega)\mu+V^{|}(\omega)\{\mu k_{\perp}^{e}(\omega)+\mu^3[k_{\|}^{e}(\omega)-k_{\perp}^{e}(\omega)]\} \qquad (5.2a)$$

$$- \frac{V^{|}(|\tilde{\omega}-\tilde{y}|)}{|\tilde{\omega}-\tilde{y}|}(\mu\omega-y)\{k_{\perp}^{e}(\omega)+\mu^2[k_{\|}^{e}(\omega)-k_{\perp}^{e}(\omega)]\}] = 0$$

and the Sym $\{\tilde{i}\tilde{j}\tilde{j} + \tilde{i}\tilde{k}\tilde{k}\}$ element is

$$\frac{3}{2}\Lambda^4[G_2+f^{|}h_3]+K_{\|}K_{\perp}^{|}+\frac{2}{y}K_{\perp}(K_{\|}-K_{\perp}) - \frac{\Lambda^2}{8}\left(\frac{V^{\|}}{y}-\frac{V^{|}}{y^2}\right)$$

$$- \frac{\Lambda^2}{8}\pi\rho\int_0^{\infty}\omega^2 d\omega\int_{-1}^{1}d\mu g(\omega)g(|\tilde{\omega}-\tilde{y}|)$$

$$X|3\{F(\omega)\mu^3+E(\omega)\mu\}+V^{|}(\omega)\{\mu[\frac{3}{2}k_{\|}^{e}(\omega)-\frac{1}{2}k_{\perp}^{e}(\omega)]$$

$$- \frac{3}{2}\mu^3[k_{\|}^{e}(\omega)-k_{\perp}^{e}(\omega)]\} \qquad (5.2b)$$

$$- \frac{V^{|}(|\tilde{\omega}-\tilde{y}|)}{|\tilde{\omega}-\tilde{y}|}(\mu\omega\{k_{\perp}^{e}(\omega)+\frac{3}{2}(1-\mu^2)[k_{\|}^{e}(\omega)-k_{\perp}^{e}(\omega)]\}$$

$$+ \frac{y}{2}\{\mu^2[k_{\|}^{e}(\omega)-k_{\perp}^{e}(\omega)]-k_{\|}^{e}(\omega)-k_{\perp}^{e}(\omega)\})] = 0$$

where

$$C(\omega) \equiv \frac{1}{2}\left(\frac{V^{\|}}{\omega} - \frac{V^{|}}{\omega^2}\right)$$

$$D(\omega) \equiv \frac{1}{6} V^{\|\|} - C$$

$$E(\omega) \equiv \frac{1}{12} V^{\|\|} - \frac{1}{6} C$$

$$F(\omega) \equiv -\frac{1}{12} V^{\|\|} + \frac{1}{2} C$$

$$G_1 \equiv h_1^{|} + \frac{2h_1}{y} - \frac{6h_3}{y}$$

$$G_2 \equiv h_3^{|} - \frac{4}{3}\frac{h_2}{y} + 4\frac{h_3}{y}$$

and $k_{\|}{}^e$ and $k_{\perp}{}^e$ are the two specific elements of $^{2\approx e}_{f}$.

All we require to solve these three equations for g, $K_{\|}$ and $K_{\perp}$ are suitable approximate expressions for h_1, h_2, and h_3 and the boundary value $K_{\|}(\infty) = K_{\perp}(\infty)$. To solve (5.1) alone for g, we need suitable approximate expressions for $K_{\|}$ and $K_{\perp}$. All this will be supplied in the following section and the Appendix.

We note that the elements of $^{4\approx}_{f}$ appear multiplied by Λ^4, and that the mean field terms in (5.2a and b) contain the factor Λ^2. As $\Lambda<0.5$ for both hydrogen and helium we find these observations reassuring.

VI. APPROXIMATE EXPRESSIONS FOR THE TENSORS

We begin with an approximate expression for the off-

diagonal portion of ρ_N:

$$\rho_N(\underset{\sim}{Y}_N, \underset{\sim}{Z}_N; \beta) \approx g_N(\underset{\sim}{Y}_N) \exp\{-\frac{2m}{\hbar^2\beta} \; {}^2\tilde{\delta} \textcircled{2} \sum_i \underset{\sim}{Z}_i^2 \qquad (6.1)$$

$$+ \sum_{i<j} [{}^2\tilde{f}^d(\underset{\sim}{y}_{ij}) \textcircled{2} \underset{\sim}{z}_{ij}^2 + {}^4\tilde{f}^d(\underset{\sim}{y}_{ij}) \textcircled{4} \underset{\sim}{z}_{ij}^4 + \ldots]\}$$

where ${}^4\tilde{f}^d$ is simply the fourth rank tensor of the dilute gas two particle density matrix at the given temperature. The first term in the exponent is the ideal gas term. It is the only one which survives in the limit of the ideal gas or in the classical limit. ${}^2\tilde{f}^d$ and ${}^4\tilde{f}^d \to 0$ as $\underset{\sim}{y}_{ij} \to \infty$. The approximation is simply that we assume that the off-diagonal effects of a non-vanishing pairwise-additive potential upon the logarithm of the N-particle density matrix are themselves pairwise-additive. This expression becomes exact in the limits of high temperature and low density.

The assumption of pairwise additivity is a common one in the statistical theory of liquids. The pairwise additivity of the potential energy is in itself an approximation, although this is often forgotten. The KSA is also an assumption of pairwise additivity of a different sort. The general reason for invoking pairwise additivity (whether it is stated or not) is that liquid theory would be intractable without it. Such is also the case here, and we are again forced to put our faith in the low densities which are typical of quantum liquids.

It is possible to show that a very similar form arises if

we assume that the system is in a pure state which may be described by a Jastrow wave function, which has been successfully applied to the study of the ground state of helium-4.[9] The only differences are that the two particle tensors are determined by the Jastrow pair factor function and that the ideal gas term does not appear.*

In the following section we shall see that the present theory is incapable of adequately describing super-fluid He^4, and that the approximation (6.1) seems to be at fault. However, the reasonable success of Jastrow function methods in describing the ground state argues that it is not the assumption of pairwise additivity per se which fails, but rather our choice of two particle tensors.

Inserting (6.1) into (3.1), which is the fundamental definition of ρ_2 in terms of ρ_N, we obtain the expression

$$\rho_2 \approx \frac{1}{V^{N-2}} \exp\left[-\frac{4m}{\hbar^2\beta}\, {}^{2}\tilde{\tilde{\delta}}\textcircled{2}\tilde{z}^2 - \frac{2\mu}{\hbar^2}\, {}^{2}\tilde{\tilde{\delta}}\textcircled{2}\tilde{z}^2 + {}^{2}\tilde{\tilde{f}}^{d}(\tilde{y})\textcircled{2}\tilde{z}^2 + {}^{4}\tilde{\tilde{f}}^{d}(\tilde{y})\textcircled{4}\tilde{z}^4\right]$$

$$\times \int d^{3N-6}\tilde{y}_N\, g_N(\tilde{y}_N) \exp\left\{\sum_{i=3}^{N}\left[{}^{2}\tilde{\tilde{f}}^{d}(\tilde{y}_{i1})\textcircled{2}\tilde{z}_1^2 + {}^{2}\tilde{\tilde{f}}^{d}(\tilde{y}_{i2})\textcircled{2}\tilde{z}_2^2 + {}^{4}\tilde{\tilde{f}}^{d}(\tilde{y}_{i1})\textcircled{4}\tilde{z}_1^4 + {}^{4}\tilde{\tilde{f}}^{d}(\tilde{y}_{i2})\textcircled{4}\tilde{z}_2^4\right]\right\}$$

where $\tilde{z}_{i1}$ and $\tilde{z}_{i2}$ have been replaced by $-\tilde{z}_1$ and $-\tilde{z}_2$, and all $\tilde{z}_i$'s and $\tilde{z}_{ij}$'s with neither i nor j equal to 1 or 2 have been set to zero.

---

*This last observation seems to support the view that Jastrow wave-function based methods are instrinsically limited to studying the ground state.

The various $^{n}\tilde{\tilde{f}}$ tensors may easily be related to the appropriate multiple gradients of the logarithm of ρ_2 by examining (3.5). Each one differs from the corresponding multiple gradient only by a numerical factor. From this point on the derivation is merely a mass exercise in partial differentiation, at the conclusion of which we set $\tilde{z}$ and $\tilde{Z}$ equal to zero. All of the resulting expressions contain three particle integrals involving g_3 which is eliminated via the usual KSA. The expressions for the fourth rank tensors also contain four particle terms involving g_4, which is eliminated via the appropriate extension of the KSA.

$$g_4(\tilde{y},\tilde{\omega},\tilde{\upsilon}) \approx g(y)g(\omega)g(\upsilon)g(|\tilde{\omega}-\tilde{y}|)g(|\tilde{\upsilon}-\tilde{y}|)g(|\tilde{\omega}-\tilde{\upsilon}|)$$

where the new variable $\tilde{\upsilon}$ is defined analogously to $\tilde{\omega}$ and is equal to $-\tilde{y}_{42}$. The final results are

$$\begin{aligned} {}^{2}\tilde{\tilde{f}}(\tilde{y}) &\approx -\frac{2\mu}{\hbar^2\beta}\,{}^{2}\tilde{\tilde{\delta}} + {}^{2}\tilde{\tilde{f}}^{d}(\tilde{y}) + {}^{2}\tilde{\tilde{f}}^{MF}(\tilde{y}) \\ &= -\frac{2\mu}{\hbar^2\beta}\,{}^{2}\tilde{\tilde{\delta}} + {}^{2}\tilde{\tilde{f}}^{d}(\tilde{y}) + \frac{n}{2}\int {}^{2}\tilde{\tilde{f}}^{d}(\tilde{\omega})g(\omega)g(|\tilde{\omega}-\tilde{y}|)d^3\tilde{\omega} \end{aligned} \tag{6.2a}$$

$${}^{2}\tilde{\tilde{f}}(\tilde{y}) = -\frac{4m}{\hbar^2\beta} + 4\,{}^{2}\tilde{\tilde{f}}^{MF}(\tilde{y}) \tag{6.2b}$$

$$\begin{aligned} {}^{4}\tilde{\tilde{f}}(\tilde{y}) &= {}^{4}\tilde{\tilde{f}}^{d}(\tilde{y}) + {}^{4}\tilde{\tilde{f}}^{MF}(\tilde{y}) \\ &= {}^{4}\tilde{\tilde{f}}^{d}(\tilde{y}) + \frac{n}{8}\int\{{}^{4}\tilde{\tilde{f}}^{d}(\tilde{\omega}) + \frac{1}{2}[{}^{2}\tilde{\tilde{f}}^{d}(\tilde{\omega})\,{}^{2}\tilde{\tilde{f}}^{d}(\tilde{\omega}) \\ &\quad + {}^{2}\tilde{\tilde{f}}^{d}(\tilde{\omega})\,{}^{2}\tilde{\tilde{f}}^{d}(\tilde{\omega}-\tilde{y})]\}g(\omega)g(|\tilde{\omega}-\tilde{y}|)d^3\omega \\ &\quad + \frac{n^2}{16}\int\int[\,{}^{2}\tilde{\tilde{f}}^{d}(\tilde{\omega})\,{}^{2}\tilde{\tilde{f}}^{d}(\tilde{\upsilon}) + {}^{2}\tilde{\tilde{f}}^{d}(\tilde{\upsilon})\,{}^{2}\tilde{\tilde{f}}^{d}(\tilde{\omega}-\tilde{y})]g(\omega)g(\upsilon) \\ &\quad \times g(|\tilde{\omega}-\tilde{y}|)g(|\tilde{\upsilon}-\tilde{y}|)[g(|\tilde{\omega}-\tilde{\upsilon}|)-1]d^3\tilde{\omega}d^3\tilde{\upsilon} \end{aligned} \tag{6.2c}$$

$$^4\tilde{\tilde{f}}(\tilde{y}) = n\int\{3\,^4\tilde{f}^d(\tilde{\omega}) + \frac{3}{2}[^2\tilde{f}^d(\tilde{\omega})]^2$$

$$- \frac{1}{2}\,^2\tilde{f}^d(\tilde{\omega})\,^2\tilde{f}^d(\tilde{\omega}-\tilde{y})\}g(\omega)g(|\tilde{\omega}-\tilde{y}|)d^3\omega$$

$$+ \frac{n^2}{2}\int\int[3\,^2\tilde{f}^d(\tilde{\omega})\,^2\tilde{f}^d(\tilde{\upsilon}) - {}^2\tilde{f}^d(\tilde{\omega})\,^2\tilde{f}^d(\tilde{\upsilon}-\tilde{y})]g(\omega)g(\upsilon)$$

$$\times\, g(|\tilde{\omega}-\tilde{y}|)g(|\tilde{\upsilon}-\tilde{y}|)[g(|\tilde{\omega}-\tilde{\upsilon}|)-1]d^3\tilde{\omega}d^3\tilde{\upsilon} \qquad (6.2d)$$

$$^4\tilde{\tilde{f}}(\tilde{y}) = 16\;{}^4\tilde{f}^{MF}(\tilde{y}) \qquad (6.2e)$$

Striking the leading terms from (6.2a and b) yields expressions for $^2\tilde{f}^c$ and $^2\tilde{\tilde{f}}^c$. If these expressions were exact, the approximation (4.6) would also be exact; this and low density are our arguments for it.

The $\tilde{y} \to \infty$ limiting values of $^2\tilde{f}$ and $^4\tilde{f}$ are

$$^2\tilde{f}(\infty) = -\frac{2\mu}{\hbar^2\beta}\,^2\tilde{\delta} + \frac{n}{2}\int{}^2\tilde{f}^d(\tilde{\omega})g(\omega)d^3\tilde{\omega} \qquad (6.3a)$$

$$^4\tilde{f}(\infty) = \frac{n}{8}\int\{^4\tilde{f}^d(\tilde{\omega}) + \frac{1}{2}[^2\tilde{f}^d(\tilde{\omega})]^2\}g(\omega)d^3\tilde{\omega}$$

$$+ \frac{n^2}{16}\int\int{}^2\tilde{f}^d(\tilde{\omega})\,^2\tilde{f}^d(\tilde{\upsilon})g(\omega)g(\upsilon)[g(|\tilde{\omega}-\tilde{\upsilon}|)-1]d^3\tilde{\omega}d^3\tilde{\upsilon} \qquad (6.3b)$$

These expressions also exhibit an unexpected smallness of the mean field terms. The mean field terms in (6.3a) and (6.3b) are, respectively, smaller by a factor of two and a factor of eight than an argument by analogy to (4.8) would lead us to expect. Also, such an argument would not predict the existence of the "cross terms" in (6.2c).

If we choose to integrate (4.5a) alone, (6.2a) provides

the needed expression for ${}^{2}\tilde{\tilde{f}}$. If we choose to integrate both (4.5a and b) together, (6.2c) provides the needed expression for ${}^{4}\tilde{\tilde{f}}$, and (6.3a), the needed expression for ${}^{2}\tilde{\tilde{f}}$ (∞).

We will have no further use for (6.2b, d and e) and (6.3b) in this paper.

In the Appendix we present scalar expressions for the specific elements of (6.2a and c) and (6.3a) which are suitable for use with the scalar equations derived in the preceding section.

VII. THE CALCULATED RESULTS FOR LIQUID He^4

Our formalism allows us to include the effects of two particle exchanges by simply calculating the required dilute gas tensors under the assumption of Bose or Fermi statistics. There is at present no way to include the effects of exchanges involving more than two particles. Except for the dotted line in Figure 4, which was calculated under the assumption of Fermi statistics, all of the results presented in this section were calculated under the assumption of Bose statistics.

Before proceeding further, we must confess to an error which crept in. We calculated the dilute gas data using $\Lambda = 0.4245$ rather than the correct value 0.4259. In the remainder of the calculation we did employ the correct value of Λ. We estimate that the error from this source is no more than about 1% and thereby considerably smaller than the error from other sources.

We begin with the rdf data in Figure 1, which refers to $\rho = 0.364$ and $T = 2.4^{o}K$. This point lies on the boundary of the liquid-gas coexistence region and is near to the λ-transition under own vapor pressure density. The experimental rdf was calculated from the X-ray scattering data of Gordon, Shaw and Daunt[10]. Three types of calculated data are presented. The best results are clearly those obtained by simultaneously integrating the three equations (5.1) and (5.2 a and b). The "one equation" results, obtained by integrating (5.1) alone are unacceptably poor, and the Mazo-Kirkwood approach results, calculated using the value $T_{eff} = 9.5^{o}K$

obtained from the three equation data, are terrible. Although the one equation results improve with increasing temperature and decreasing density, neither of the two simpler approaches yields acceptable results anywhere in the region $T < 10^{o}K$, $\rho \geq 0.311$ and we will not consider them further in this section.

The slight discrepancy between the three equation and experimental rdf's at $y = 0.9$ is due to an experimental artifact. The discrepancy at $y \geq 1.3$ is more significant. It may best be described as a shift in the phase of the peaks of the rdf. In order to explain its origin we turn to Figure 2. Here we present the experimental and three equation values of the quantity $4\pi R^2 n\,[g(R) - 1]$, where n is the number density and R the interatomic separation in $\mathring{A}$. The experimental values are the neutron scattering results of Henshaw[11], and are for $\rho = 0.462$ and $T = 4.2^{o}K$. The calculated results are for $\rho = 0.467$, $T = 4.5^{o}K$ and $T_{eff} = 15.2^{o}K$. This density is slightly above the normal fluid superfluid-solid triple point density of $\rho \approx 0.455$. Presenting the rdf's multiplied R^2 makes the small outer peaks and troughs clearly visible, and the higher density accentates the error which we wish to examine. The oscillations in the experimental curve are seen to decrease rather slowly with R. The oscillations in the calculated curve die down much more rapidly and disappear completely at $11\mathring{A}$ or, equivalently $y = 4.3$. The phase shift of the peaks is seen to be the result of this overly rapid decay.

In our calculations we arbitrarily set the rdf equal to unity for $y \geq 4.3$ and actually integrated the equations only for $y < 4.3$. This approximation seems to be the origin of most of the discrepancy. We believe that removing this approximation would, at least at the lower densities, render the agreement with experiment almost perfect. Until this is done, it would be futile to try to calculate the isothermal compressibility which depends critically on the rdf at large y, and we have not attempted this calculation.

More calculated rdf data for various temperatures and densities is presented in Tables 2-4, along with the values of the elements of $^2\tilde{f}$ and $^4\tilde{f}$. Instead of directly presenting the values of $k_{||}$ and $k_{\perp}$ or $K_{||}$ and $K_{\perp}$, we have chosen to tabulate the "effective temperatures"

$$T_{||} \equiv 2 \left(\frac{\epsilon}{k_B}\right) K_{||} \text{ or } \perp$$

Comparing Tables 2 and 3 reveals that the rdf and the elements of $^4\tilde{f}$ are only weakly temperature dependent. It is possible to determine that the same is true of $\Delta T_{||} \equiv T_{||} - T_{||}(\infty)$ and $\Delta T_{\perp}$. It is easy to explain this in a physically intuitive manner: Liquid helium is so quantum mechanical that "zero-point" effects largely overwhelm thermal effects.

We present calculated pressure and internal energy data in Figures 3 and 4. This data is for $\rho = 0.380$, which is slightly above the normal λ- point and thus in the region of greatest

interest. The experimental data for $T \geqslant 3^{o}K$ is taken from Hill and Lounasmaa[12] and below $3^{o}K$, from Lounasmaa[13].

The reference state for the internal energy is the infinitely dilute gas at absolute zero. (This is 59.5j/mole above the reference state employed by Hill and Lounasmaa[12] and Lounasmaa [13].) In Figure 4 we also present internal energy data calculated under the assumption of Fermi statistics as the comparison is instructive. Above the λ-temperature the Bose calculated curve is in good agreement with experiment and above $3^{o}K$, the effect of statistics is small. Unfortunately, below the λ-temperature the Bose curve drops off more and more rapidly with decreasing temperature instead of quickly going to a low temperature limit as do the experimental values. The Fermi curve goes through a minimum at the λ-temperature and begins to increase again, which is absurd. The theory clearly collapses at the λ-transition, and the collapse is apparently due to its present inability to deal with exchanges involving more than two particles. All this is consistent with the Bose-Einstein condensation theory of the λ-transition, as it indicates that above the λ-temperature only two particle exchanges are important, while exchanges involving more particles suddenly become important at and below the transition. The low temperature collapse of the Fermi results bodes ill for any attempt to apply the theory in its present form to helium-3, although the very low densities which are typical of helium-3 might save the situation somewhat.

The low temperature statistical effects evident in the calculated data of Figure 4 enter through the kinetic energy term of the internal energy. In both cases the calculated potential energy proved to be virtually temperature independent. (The Bose value of the potential energy is calculated to be -174.60 ± 0.05j/mole for $1.9^{o}K < T < 4.4^{o}K$.)

In Figure 5 we present the calculated values of the quantity $T_{eff} - T$ for four densities. A slight maximum is apparent in the $\rho = 0.380$ curve at $T \sim 2.7^{o}K$. This maximum is demonstrably the source of the low temperature behavior of the calculated Bose internal energy. The $\rho = 0.467$ curve exhibits a less pronounced maximum at $T \sim 2.4^{o}K$. It is tempting to identify these maxima as indications of the proximity of the λ-transition. (The higher density is actually slightly above the superfluid range of densities, but we may well expect the theory to be insensitive to this fine distinction.) The shift to lower temperature with increasing density is consistent with this interpretation.

In Figure 6 we present the values of $h_1(\infty) = h_2(\infty) = 3h_3(\infty)$ at the same four densities. The virtual temperature independence is striking.

We close this section with a brief comparison of our results with the recent ground state results of Kalos, Levesque and Verlet[14] which appear to be the best ground state results available. Using two different methods, they calculated the effective temperature

of the ground state under zero pressure (ρ = 0.3648) to be 11.9 $\pm$ 0.1°K. (These authors define the effective temperature somewhat differently. 11.9°K is actually two-thirds of their differently defined value.) We can compare this value with our calculated effective temperatures for ρ = 0.364. We do not explicitly present the ρ = 0.364 data, but the interested reader may construct it from the ρ = 0.380 curve of Figure 5 by noting that T_{eff} (0.364) $\approx$ T_{eff} (0.380) -0.6°K. (Please note that here we are discussing T_{eff} rather than T_{eff} - T.)

For ρ = 0.364, our calculations indicate that T_{eff} = 11.9°K corresponds to T $\sim$ 4.8°K and that T_{eff} $\sim$ 9.3°K near the λ-transition. This seems to indicate a minimum in the effective temperature (or, equivalently, the average kinetic energy per particle) at constant density at or below the λ-transition temperature. It seems safe to guess that it is at or very near the λ-transition. The validity of this conclusion rests upon the accuracy of both calculations. The KLV result does actually seem to be about 0.9°K too high, but correcting this merely reduces the depth of the minimum to about 1.7°K. We believe that our calculated effective temperatures are accurate to considerably better than 1.7°K and thereby accept the physical existence of the minimum. This minimum explains the well known maximum in the density at constant pressure very near the λ-transition.

VIII. CALCULATED RESULTS FOR LIQUID p-HYDROGEN

Para-hydrogen molecules are essentially all in the ground

state when $T < 50^{o}K$, but at higher temperatures, rotational excitations make a significant contribution to the internal energy. Before presenting our p-H_2 results, we briefly describe how we calculated this contribution.

Using data and formulas given by Davidson[15], we calculate the difference between the $J = 0$ and $J = 2$ rotational energies as being 4365.2j/mole or, equivalently, $525^{o}K\ xk_B$. The gap between the $J = 2$ and $J = 4$ states is even greater, and it is clear that the only rotationally excited state which will contribute significantly is $J = 2$.

Recalling that the $J = 2$ state is fivefold degenerate, we write the contribution of rotational excitations as

$$E_{rot}\ (j/mole) = \frac{21826\ \exp\ (-525/T)}{1 + 5\ \exp\ (-525/T)}$$

This quantity varies from $\sim$ 100j/mole at 100K down to <1j/mole below $50^{o}K$. At $100^{o}K$ about 2.5% of the molecules are in the $J = 2$ state. We make no attempt to account for the lack of spherical symmetry of the excited molecules, as this effect is doubtlessly minute due to their small concentration.

We will focus primarily upon data for $\rho = 0.575$ (approximately the liquid density at the triple point) and make occassional mention of data for $\rho = 0.401$ (a density about midway between the critical and triple point densities) and at $\rho = 0.234$ (the critical point density).

Most of the p-H_2 results presented in this section were

calculated via both the three equation - approach and the one equation approach. The difference between the two sets of results is everywhere small, in marked contrast to the case of He^4. For the most part we present the three equation results as they are more informative. The main exception are the one equation results which we present for $\rho = 0.575$ and $T < 30^oK$. In this region we were unable to obtain satisfactory convergence in the three equation calculations with a reasonable expenditure of effort. However, the one equation approach did converge in this region and gave satisfactory results. This fact along with other considerations lead us to believe that the non-convergence of the three equation calculation in this region was due to numerical instability rather than being indicative of the impending collapse of the theory. We (correctly) employed dilute gas data calculated under the assumption of Bose statistics although statistical effects proved to be negligibly small.

We also present some data obtained by applying the YBG equation in a purely classical manner and ignoring the contributions of rotational excitations. We compare these results with experimental data on argon which has been rescaled via the law of corresponding states to make it refer to a hypothetical classical liquid which has the same intermolecular potential parameters as p-H_2. This data allows us to conveniently examine the magnitude of the quantum effects and to compare the quality of our calculated results for

p-H_2 with that observed when the classical YBG equation is applied to argon.

All of the experimental data on para-hydrogen is taken from the massive compilation of Roder, Weber and Goodwin.[16] All argon data is from the compilation of Levelt.[17]

We begin with the rdf results of Figures 7 and 8. Unfortunately, we were not able to find any experimental data with which to compare our calculated rdf's. X-ray scattering is difficult because of the small scattering cross-section and neutron scattering is complicated by the possibility of rotational excitations at the shorter wavelengths. We can only hope that our results will encourage someone to correct this deficiency.

Figure 7 refers to $\rho = 0.401$ and $T = 31^{o}K$. This point is just above the boundary of the liquid-gas coexistence region in temperature and $T_{eff} = 46.8^{o}K$. The Mazo-Kirkwood rdf is typically that of a classical fluid. In contrast to this, the three equation rdf has much less pronounced maxima, and they occur at greater separations. At the collision diameter, the three equation rdf is ~ 0.7. In the region $y < 1$ considerable tunnelling is evident, and the second maximum is prominent only because of the deep minimum adjacent to it. As anticipated, this rdf has an appearance intermediate between those of helium and classical fluids. The differences between the Mazo-Kirkwood and three equation rdf's grow more pronounced at lower densities, where the three equation rdf becomes exact and

and the Mazo-Kirkwood rdf grows even worse. We also present the rdf of the dilute gas at the same temperature. The maximum of this rdf is more pronounced than the first maximum of the three equation rdf because the thermodynamic temperature is considerably smaller than the effective temperature.

Figure 8 refers to a point at roughly the triple point density and about 19°K above it in temperature. $T_{eff} = 58.4^{o}K$. We see that going to a higher density reduces the discrepancy between the MK rdf and the three equation rdf but does not eliminate it. This improvement is due to the fact that at higher densities the mean field kinetic energy effects tend to predominate, thereby improving the validity of Mazo and Kirkwood's fundamental assumption.

Figure 8 refers to the lowest temperature at which we completely trust the three equation results at $\rho = 0.575$. Therefore, we have chosen it to compare the three equation and one equation results. The difference is seen to be rather small. Furthermore, it decreases rapidly with increasing temperature and decreasing density.

Tables 5 and 6 present the three equation data of Figures 7 and 8 in tabular form along with the values of the elements of $\overset{\approx}{f}^{2}$ and $\overset{\approx}{f}^{4}$. Table 7 presents one equation rdf and $\overset{\approx}{f}^{2}$ data at a point which is very slightly above the triple point in temperature. Again the elements of $\overset{\approx}{f}^{2}$ are presented in the form of $T_{\parallel}$ and $T_{\perp}$

The general impression given by the calculated rdf's and the elements of $\tilde{f}^{422}$ is one of very weak temperature dependence as was observed in the case of He^4. $\Delta T_{||}$ and $\Delta T_{\perp}$ may also be determined to be weakly temperature dependent. The difference between the rdf's in Tables 6 and 7 is due mostly to the fact that Table 6 contains three equation results and Table 7 one equation results. The one equation rdf at the temperature and density of Table 6 (which is presented in Figure 8) is nearly identical to the rdf of Table 7, but its peaks are slightly more pronounced despite the higher temperature. This physically unreasonable increase of structure with increasing temperature is exhibited by the p-H_2 one equation approach results only for $\rho = 0.575$, $T < 30^{\circ}K$. It is not exhibited by the lower density p-H_2 or He^4 data. It is, however, pronounced in the generally ill-fated He^4 one equation results. We are forced to conclude that this behavior indicates that the one equation approach is near its limit of utility under these extreme conditions of temperature and density.

In Figures 9 and 10 we present the values of T_{eff} and h_1 (∞) at three densities. The weak temperature dependence of the "quantum effects" is striking, as is the ratio T_{eff} to T in the vicinity of the triple point.

Figures 11 and 12 compare our calculated results for the internal energy and pressure at $\rho = 0.575$ with experiment. We also present rescaled experimental data for argon and compare it with

results generated using the classical YBG equation. In Figure 11 we also present our calculated values of the kinetic energy. The agreement between the one equation and three equation results is excellent. In particular, the one equation curves of Figure 11 would merge almost perfectly with the three equation curves if we were to extend them to higher temperature. In Figure 12 the quality of the agreement of the p-H_2 energy values with experiment is better than that of the classically calculated argon values. The genesis of the present theory as an extension of the YBG equation to quantum liquids is clearly evidenced. The quality of the p-H_2 and argon results is roughly equal at lower densities.

IX. CONCLUSION

In the preceeding section we demonstrated that the quality of our results for p-H_2 at $\rho = 0.575$ is reasonably good and comparable to that observed when the classical YBG equation is applied to liquid argon. However, $\rho = 0.575$ is in the density range of greatest interest in the case of ρ-H_2 while it is only about midway between the critical and triple point liquid densities in the case of argon. For this reason we feel justified in considering our p-H_2 results to actually be better. In Section 7 we saw that the three equation approach also yielded a satisfactory description of normal liquid helium-4. And so it seems that the "first guess" theories presented here have proven themselves to be fairly successful when properly applied, although this is certainly not the case with the analagous classical YBG theory.

This is, of course, due to the lower densities typical of quantum liquids. We anticipate that this fact will prove equally beneficial to the future development of more sophisticated theories of simple quantum fluids.

The fact that the one equation approach gives essentially the same results for p-H_2 as does the considerably more complex three equation approach has important implications. The fundamental difference between the two approaches is in the way that approximation (6.1) enters into them. The one equation approach utilizes only the second rank portion of (6.1), and utilizes it rather directly. The three equation approach utilizes both the second and fourth rank portions of (6.1) but in a rather less direct manner. Also, the "mean field dimunition" and "multiplication by powers of Λ" effects pointed out in Sections 4, 5 and 6 are powerfully evident in the three equation approach but much less pronounced in the one equation approach. (They would be even more pronounced in higher order approaches.) Now, there is no reason to expect the fourth rank portion of approximation (6.1) to be any better than the second rank portion. We believe that the reason that the three equation approach succeeds in the case He^4 while the one equation approach fails is that the various benefits of the three equation approach are capable of overwhelming the fundamental shortcomings of applying (6.1) to this highly quantum mechanical substance. In the case of p-H_2, how-

ever, the one equation approach is not significantly worse, and it seems that the benefits of the three equation approach are not essential. We believe that this indicates that the second rank portion of approximation (6.1) is sufficiently accurate to serve as a starting point for treating liquid p-H_2 and all liquids of equal or less pronounced quantum mechanical character. The slight improvements to be expected from employing the three equation approach can probably be achieved by appending some reasonably simple perturbation scheme onto the intrinsically simple and convenient one equation approach or its future analogues.

ACKNOWLEDGEMENTS

I would like to thank the Miller Institute for Research in Basic Science for providing me with the Fellowship support which made this work possible, and William H. Miller for generously supplying me with computer time. His patience held up even though my several estimates of how much more I would require did not. Also, many thanks for stimulating discussions and incisive questions to Berni J. Alder, who does not allow an approximation to slip by unexamined.

In deepest sorrow, I dedicate this work to Rick Abramson who did not live to see it completed. His persistent encouragement and interest helped me enormously.

APPENDIX

In this appendix we present scalar expressions for the specific elements of the approximate expressions for $2\tilde{\tilde{f}}$ and $4\tilde{\tilde{f}}$ which we derived in Section 6. We present only the final results.

$$K_{||}(y) = \frac{1}{2t} - \frac{\Lambda^2}{2}\left[k_{||}^{d}(y) + \pi\rho\int_0^\infty \omega^2 d\omega \int_{-1}^{1} d\mu g(\omega) g\left(\sqrt{y^2 + \omega^2 - 2y\omega\mu}\right)\right.$$

$$\left.\left\{k_{\perp}^{d}(\omega) + \mu^2\left[k_{||}^{d}(\omega) - k_{\perp}^{d}(\omega)\right]\right\}\right] \qquad \text{(A1a)}$$

$$K_{\perp}(y) = \frac{1}{2t} - \frac{\Lambda^2}{2}\left[k_{\perp}^{d}(y) + \pi\rho\int_0^\infty \omega^2 d\omega \int_{-1}^{1} d\mu g(\omega) g\left(\sqrt{y^2 + \omega^2 - 2y\omega\mu}\right)\right.$$

$$\left.\left\{k_{\perp}^{d}(\omega) + \frac{1}{2}(1-\mu^2)\left[k_{||}^{d}(\omega) - k_{\perp}^{d}(\omega)\right]\right\}\right] \qquad \text{(A1b)}$$

where $k_{||}{}^{d}$ and $k_{\perp}{}^{d}$ are the two specific elements of $2\tilde{\tilde{f}}^{d}$.

$$K_{||}(\infty) = K_{\perp}(\infty)$$

$$= \frac{1}{2t} - \frac{\pi\rho\Lambda^2}{3}\int_0^\infty \omega^2 d\omega g(\omega)\left[k_{||}^{d}(\omega) + 2k_{\perp}^{d}(\omega)\right] \qquad \text{(A2)}$$

We present the expressions for the elements of $4\tilde{\tilde{f}}$ as the elements of a formal vector

$$\tilde{h} = \tilde{i}\, h_1 + \tilde{j}\, h_2 + \tilde{k}\, h_3$$

This notation is compact and well suited for numerical implementation.

$$\tilde{h}(y) = \tilde{h}^d(y) + \frac{\pi\rho}{4}\int_0^\infty \omega^2 d\omega \int_{-1}^{1} d\mu \Big[\tilde{\tilde{T}}_2(\mu)\cdot\tilde{h}^a(\omega)$$

$$+ \frac{1}{2}\tilde{\tilde{T}}_2'(\mu,\omega,y)\cdot\tilde{A}_2(\mu,\omega,y)\Big]\, g(\omega)\, g(|\tilde{y}-\tilde{\omega}|)$$

$$+ \frac{\pi\rho^2}{4}\int_0^\infty \upsilon^2 d\upsilon \int_0^\infty \omega^2 d\omega \int_{-1}^{1} d\mu_\upsilon \int_{-1}^{1} d\mu_\omega \int_0^\pi d\phi \qquad \text{(A3)}$$

$$\times \Big\{ [g(|\tilde{\omega}-\tilde{\upsilon}|)-1]\,\tilde{\tilde{T}}_5(\mu_\upsilon,\mu_\omega,\phi) + [g(d)-1]\,\tilde{\tilde{T}}_5'(\mu_\upsilon,\mu_\omega,\phi)\Big\}$$

$$\cdot A_5(\upsilon,\omega)\, g(\upsilon) g(\omega)\, g(|\tilde{\upsilon}-\tilde{y}|) g(|\tilde{\omega}-\tilde{y}|)$$

where $\phi \equiv \phi_\omega - \phi_\upsilon$ and $\tilde{h}^d$ is the vector composed of the dilute gas values of h_1, h_2 and h_3:

$$\tilde{h}^d = \tilde{i}\, h_1^d + \tilde{j} h_2^d + \tilde{k} h_3^d$$

the elements of $\tilde{h}^a$ are

$$h_1^a \equiv h_1^d + \frac{1}{2}(k_{||}^d)^2$$

$$h_2^a \equiv h_2^d + \frac{1}{2}(k_\perp^d)^2$$

$$h_3^a \equiv h_3^d + \frac{1}{6} k_{||}^d k_\perp^d$$

$$\tilde{\tilde{T}}_2(\mu) = \begin{vmatrix} \mu^4 & 1-2\mu^2+\mu^4 & 6\mu^2-6\mu^4 \\ \frac{3}{8} - \frac{3}{4}\mu^2 + \frac{3}{8}\mu^4 & \frac{3}{8} + \frac{1}{4}\mu^2 + \frac{3}{8}\mu^4 & \frac{3}{4} + \frac{3}{2}\mu^2 - \frac{9}{4}\mu^4 \\ \frac{1}{2}\mu^2 - \frac{1}{2}\mu^4 & \frac{1}{6} + \frac{1}{3}\mu^2 - \frac{1}{2}\mu^4 & \frac{1}{2} - \frac{5}{2}\mu^2 + 3\mu^4 \end{vmatrix}$$

$$\overset{\approx}{T}_5\ (\mu\upsilon,\mu\omega,\phi) = \begin{vmatrix} 1 & \mu_\omega^2 & \mu_\upsilon^2 & \mu_\upsilon^2\,\mu_\omega^2 \\ 1 & \frac{1}{2}S_\omega^2 & \frac{1}{2}S_\upsilon^2 & (\frac{1}{4}+\frac{1}{8}C_{2\phi})S_\upsilon^2 S_\omega^2 \\ \frac{1}{3} & \frac{1}{12}+\frac{1}{12}\mu_\omega^2 & \frac{1}{12}+\frac{1}{12}\mu_\upsilon^2 & \frac{1}{3}C_\phi\,\mu_\upsilon\mu_\omega S_\upsilon S_\omega \\ & & & +\frac{1}{12}[\mu_\upsilon^2 S_\omega^2+\mu_\omega^2 S_\upsilon^2] \end{vmatrix}$$

where $C_\phi \equiv \cos\phi$, $S_\upsilon \equiv \sin\theta_\upsilon = 1 - \mu_\upsilon^2$, and so on.

$\overset{\approx}{T}_5'$ differs from $\overset{\approx}{T}_5$ only in the sign of the first term of the (3,4) or lower right corner element.

$$\tilde{A}\ (\upsilon,\omega) = \begin{vmatrix} k_\perp^d(\upsilon)\,k_\perp^d(\omega) \\ k_\perp^d(\upsilon)\,[\,k_{||}^d(\omega) - k_\perp^d(\omega)\,] \\ k_\perp^d(\omega)\,[\,k_{||}^d(\upsilon) - k_\perp^d(\upsilon)\,] \\ [k_{||}^d(\upsilon) - k_\perp^d(\upsilon)\,]\,[k_{||}^d(\omega) - k_\perp^d(\omega)\,] \end{vmatrix}$$

$\overset{\approx}{T}_2'$ and $\tilde{A}_2$ are obtained by inserting

$$C_\phi = C_{2\phi} = \cos(0) = 1$$

$$\upsilon = |\,\tilde{\omega} - \tilde{y}\,|$$

$$\mu_\upsilon = \frac{1}{\upsilon}(\omega\mu - y)$$

into the expressions for $\overset{\approx}{\tilde{T}}_5$ and $\tilde{A}_5$.

$$d \equiv | \tilde{\omega} - 2\tilde{\iota\omega}\, \mu_\omega\, -\tilde{\upsilon} + \tilde{y} |$$

The form in which we have written the second term of the five dimensional integrand in (A3), which involves $\overset{\approx}{T}_5$, and d, is not that which is obtained by reducing (6.2c) to its specific elements in the most direct way. It is the result of some additional manipulations, and leads to significant computational economies.

BIBLIOGRAPHY

1. R. M. Mazo, J. G. Kirkwood, Proc. Nat. Acad. Sci. USA 41 (1955) 204, R. M. Mazo, J. G. Kirkwood, Phys. Rev. 100 (1955) 1787, R. M. Mazo, J. G. Kirkwood, J. Chem. Phys. 28 (1958) 644.

2. T. B. Drew, "Handbook of Vector and Polyadic Analysis," Reinhold Publishing Corp. (New York , 1961) pp. 21-27.

3. E. Wigner, Phys. Rev. 40 (1932) 749.

4. H. Crámer, "Mathematical Methods of Statistics," Princeton University Press (Princeton, 1946) p. 185.

5. R. P. Feynmann and A. R. Hibbs, "Quantum Mechanics and Path Integrals," McGraw Hill, Inc. (New York, 1965) pp. 275-6.

6. N. N. Bogoliubov, "Lectures on Quantum Statistics," Vol. I, trans. from Ukrainian, edited by L. Klein and S. Glass, Gordon and Breach (New York, 1967)p. 19.

7. G. K. Batchelor, "Theory of Homogeneous Turbulence," Cambridge University Press (Cambridge, 1953) pp. 40-45.

8. N. N. Bogoliubov, op. cit. pp. 17-31.

9. W. L. McMillan, Phys. Rev. 138 (1965) A442, D. Schiff and L. Verlet, Phys. Rev. 160 (1967) 208, W. P. Francis, G. V. Chester and L. Reatto, Phys. Rev. A1 (1970) 86.

10. W. L. Gordon, C. H. Shaw, and J. G. Daunt, J. Phys. Chem. Solids, 5, (1958) 117.

11. D. G. Henshaw, Phys. Rev. 119 (1960) 14.

12. R. W. Hill and O. V. Lounasmaa, Phil. Trans. Roy. Soc. (London), A252 (1960) 357.

13. O. V. Lounasmaa, Cryogenics, 1 (1961) 212.

14. M. H. Kalos, D. Levesque and L. Verlet, Phys. Rev. A9 (1974) 2178.

15. N. Davidson, "Statistical Mechanics," McGraw Hill, Inc. (New York, 1962) pp. 110-119.

16. H. M. Roder, L. A. Weber and R. D. Goodwin, "Thermodynamic and Related Properties of Parahydrogen from the Triple Point to 100°K at Pressures to 340 Atmospheres," U.S. Nat. Bur. Stand. Monograph 94 (Washington, 1965) pp. 73-107

17. J. M. H. Levelt, Physica 26 (1960) 361.

TABLE 1

	σ (Å)	$\frac{\epsilon}{k_B}$ (^oK)	μ (g x 10^{-24})	Λ
He^4	2.556	10.22	3.322	0.4259
p-H_2	2.928	37.0	1.673	0.2753

TABLE 2

He^4, $\rho = 0.380$, $T = 2.4^oK$

y	g	$T_{\|\|}$	$T_\perp$	h_1	h_2	h_3
0.8	-	246.7	-17.1	-9.42(2)*	-5.15(1)	1.57(2)
0.9	0.13	113.0	-0.1	-3.41(2)	-1.55(1)	5.69(1)
1.0	0.47	55.4	6.1	-1.32(2)	-3.48	2.21(1)
1.1	0.91	29.8	8.4	-5.56(1)	0.57	9.40
1.2	1.25	17.8	9.2	-2.48(1)	2.02	4.39
1.3	1.39	12.2	9.6	-1.12(1)	2.56	2.29
1.4	1.34	9.9	10.0	-4.59	2.80	1.41
1.5	1.18	9.4	10.2	-1.12	2.87	1.04
1.6	1.01	9.9	10.3	0.93	2.83	0.88
1.7	0.90	10.5	10.3	2.25	2.75	0.83
1.8	0.84	11.0	10.2	3.13	2.67	0.81
1.9	0.83	11.3	10.2	3.66	2.63	0.81
2.1	0.91	11.1	10.1	3.67	2.65	0.86
2.3	1.04	10.3	10.0	3.06	2.69	0.90
2.5	1.06	9.9	10.1	2.65	2.75	0.91
2.7	1.00	10.0	10.1	2.67	2.79	0.94
∞	-	10.2	10.2	2.74	2.74	0.91

*Indicates exponent; i.e., - 9.42 (2) = - 942.

TABLE 3

He^4, $\rho = 0.380$, $T = 7.9^oK$

y	g	$T_{\|\|}$	$T_{\perp}$	h_1	h_2	h_3
0.8	-	247.7	-12.3	-9.42(2)	-4.83(1)	1.54(2)
0.9	0.16	114.6	4.6	-3.41(2)	-1.38(1)	5.45(1)
1.0	0.55	57.5	10.9	-1.32(2)	-2.53	2.04(1)
1.1	1.00	32.3	13.2	-5.49(1)	1.09	8.29
1.2	1.30	20.8	14.2	-2.37(1)	2.32	3.66
1.3	1.37	15.7	14.7	-9.97	2.73	1.84
1.4	1.28	13.8	15.1	-3.39	2.88	1.14
1.5	1.14	13.6	15.3	0.01	2.89	0.89
1.6	1.01	14.0	15.4	1.88	2.82	0.81
1.7	0.94	14.6	15.3	2.99	2.75	0.82
1.8	0.90	15.1	15.2	3.68	2.69	0.84
1.9	0.90	15.4	15.0	4.04	2.68	0.87
2.1	0.96	15.4	14.8	3.66	2.73	0.93
2.3	1.03	15.0	14.8	2.78	2.77	0.94
2.5	1.03	14.8	14.9	2.37	2.80	0.93
2.7	1.00	14.8	15.0	2.57	2.81	0.93
∞	-	14.8	14.8	2.79	2.79	0.93

TABLE 4

He^4, $\rho = 0.467$, $T = 2.4^oK$

y	g	$T_{\|\|}$	$T_{\perp}$	h_1	h_2	h_3
0.8	-	247.1	-11.3	-9.42(2)	-4.97(1)	1.57(2)
0.9	0.17	113.7	4.5	-3.41(2)	-1.38(1)	5.72(1)
1.0	0.59	56.3	10.1	-1.32(2)	-2.13	2.23 (1)
1.1	1.11	31.0	12.0	-5.53(1)	1.72	9.61
1.2	1.46	19.5	12.8	-2.43(1)	3.15	4.62
1.3	1.52	14.5	13.2	-1.04(1)	3.73	2.58
1.4	1.36	12.9	13.5	-3.53	4.09	1.77
1.5	1.14	13.1	13.7	0.16	4.16	1.45
1.6	0.96	13.9	13.6	2.42	3.99	1.28
1.7	0.86	14.7	13.5	3.90	3.77	1.20
1.8	0.82	15.2	13.4	4.89	3.62	1.15
1.9	0.83	15.4	13.4	5.39	3.58	1.13
2.1	0.96	14.8	13.2	5.15	3.70	1.24
2.3	1.10	13.5	13.3	4.33	3.74	1.27
2.5	1.05	13.5	13.6	3.60	3.84	1.26
2.7	0.97	13.7	13.6	3.81	3.86	1.31
∞	-	13.6	13.6	3.75	3.75	1.25

TABLE 5

$p\text{-}H_2$, ρ = 0.401, T = 31.0°K

y	g	$T_{\|\|}$	$T_{\perp}$	h_1	h_2	h_3
0.8	-	577.6	-8.1	-1.45(3)	-6.53(1)	2.32(2)
0.9	0.13	267.7	28.6	-5.25(2)	-1.49(1)	8.09(1)
1.0	0.69	136.1	41.4	-2.01(2)	0.66	2.95(1)
1.1	1.38	79.6	45.6	-8.17(1)	5.15	1.16(1)
1.2	1.66	55.3	47.1	-3.28(1)	6.47	5.12
1.3	1.54	46.1	47.9	-1.08(1)	6.78	2.82
1.4	1.31	43.8	48.3	-0.35	6.88	2.15
1.5	1.11	44.3	48.5	4.58	6.82	2.05
1.6	0.99	45.7	48.4	6.84	6.66	2.06
1.7	0.92	47.2	48.0	7.96	6.42	2.10
1.8	0.89	48.3	47.6	8.80	6.31	2.14
1.9	0.91	48.9	47.1	9.59	6.35	2.23
2.1	1.01	48.8	46.6	8.67	6.62	2.33
2.3	1.07	47.4	46.7	5.97	6.62	2.21
2.5	1.05	46.8	47.0	5.26	6.62	2.15
2.7	1.01	47.0	47.2	6.15	6.55	2.15
∞	-	46.8	46.8	6.40	6.40	2.13

TABLE 6

$p\text{-}H_2$, ρ = 0.575 T = 33.5°K

y	g	$T_{\|\|}$	$T_{\perp}$	h_1	h_2	h_3
0.8	-	579.6	7.9	-1.45(3)	-6.04(1)	2.32(2)
0.9	0.17	270.4	41.9	-5.23(2)	-1.12(1)	8.11(1)
1.0	0.85	139.9	53.4	-1.99(2)	3.45	2.98(1)
1.1	1.59	85.0	57.1	-7.93(1)	7.31	1.21(1)
1.2	1.77	62.9	58.7	-2.98(1)	8.53	5.74
1.3	1.54	55.8	59.6	-7.28	8.88	3.64
1.4	1.25	55.0	60.0	3.40	9.35	3.20
1.5	1.04	56.5	60.0	8.55	9.48	3.21
1.6	0.91	58.5	59.7	1.09(1)	9.22	3.15
1.7	0.84	60.6	59.2	1.18(1)	8.71	3.05
1.8	0.83	62.2	58.6	1.26(1)	8.63	3.03
1.9	0.88	62.6	58.1	1.39(1)	8.95	3.19
2.1	1.03	61.5	57.7	1.15(1)	9.70	3.32
2.3	1.09	59.5	58.5	7.07	9.52	3.06
2.5	1.04	59.0	59.1	6.83	9.46	3.04
2.7	0.98	59.2	59.1	9.07	9.36	3.09
∞	-	58.4	58.4	9.29	9.29	3.10

TABLE 7

$p\text{-}H_2$, $\rho = 0.575$, $T = 14.6°K$

y	g	$T_{\|\|}$	$T_{\perp}$
0.8	-	587.1	-31.0
0.9	0.15	274.8	15.2
1.0	0.72	141.5	33.3
1.1	1.36	83.0	40.4
1.2	1.61	56.2	43.1
1.3	1.52	43.8	44.2
1.4	1.31	38.4	44.5
1.5	1.12	36.6	44.6
1.6	0.97	36.9	44.5
1.7	0.89	38.4	44.4
1.8	0.87	40.4	44.2
1.9	0.89	42.6	43.9
2.1	0.99	45.7	43.5
2.3	1.06	44.9	43.4
2.5	1.05	43.3	43.4
2.7	1.01	42.5	43.5
∞	-	43.2	43.2

FIGURE CAPTIONS

Figure 1 Calculated and experimental rdf's of He^4 at $\rho = 0.364$ and 2.4^oK. Open circles, experimental. Heavy solid line, three equation results. Light solid line, one equation results. Dashed line, Mazo-Kirkwood approach results.

Figure 2 The quantity $4\pi R^2 n\,[g(R) - 1\,]$ for He^4. Open circles, experimental values for $\rho = 0.462$ and 4.2^oK. Solid line, three equation results for $\rho = 0.467$ and 4.5^oK.

Figure 3 Experimental and calculated pressure of He^4 for $\rho = 0.380$. Open circles, experimental. Solid line, three equation results.

Figure 4 Experimental and calculated internal energies of He^4 for $\rho = 0.380$. Open circles, experimental. Solid line, three equation results with assumption of Bose statistics. Dashed line, three equation results with assumption of Fermi statistics. Λ temperature indicated.

Figure 5 Three equation values of T_{eff} -T of He^4 at various densities. c.p. = critical point. l-v = liquid vapor coexistence boundary. λ = λ-line. s-l = solid-liquid II coexistence boundary.

Figure 6 Three equation values of h_1 (∞) of He^4 at same densities as in Figure 5.

Figure 7 Calculated rdf's of p-H_2 at ρ = 0.401 and 31°K. Heavy solid line, three equations. Dashed line , Mazo-Kirkwood approach. Light solid line, dilute gas result.

Figure 8 Calculated rdf's of p-H_2 of ρ = 0.575 and 33.5°K. Heavy solid line, three equations. Light solid line, one equation. Dashed line, Mazo-Kirkwood approach.

Figure 9 Calculated effective temperature of p-H_2 vs. thermodynamic temperature at three densities. Dashed line, classical limiting value. Low temperature portion of ρ = 0.575 curve from one equation, rest of data from three equations.

Figure 10 $h_4^*(\infty)$ of p-H_2 vs. thermodynamic temperature for three densities. The classical limiting value is zero. All data from three equation calculation.

Figure 11 Internal and kinetic energies of p-H_2 and Ar at ρ = 0.575. Open circles, experimental. Solid lines, calculated. p-H_2 data calculated from one equation, light line. Argon data rescaled as described.

Figure 12 Pressures of p-H_2 and Ar at ρ = 0.575. Same representation as Figure 11.

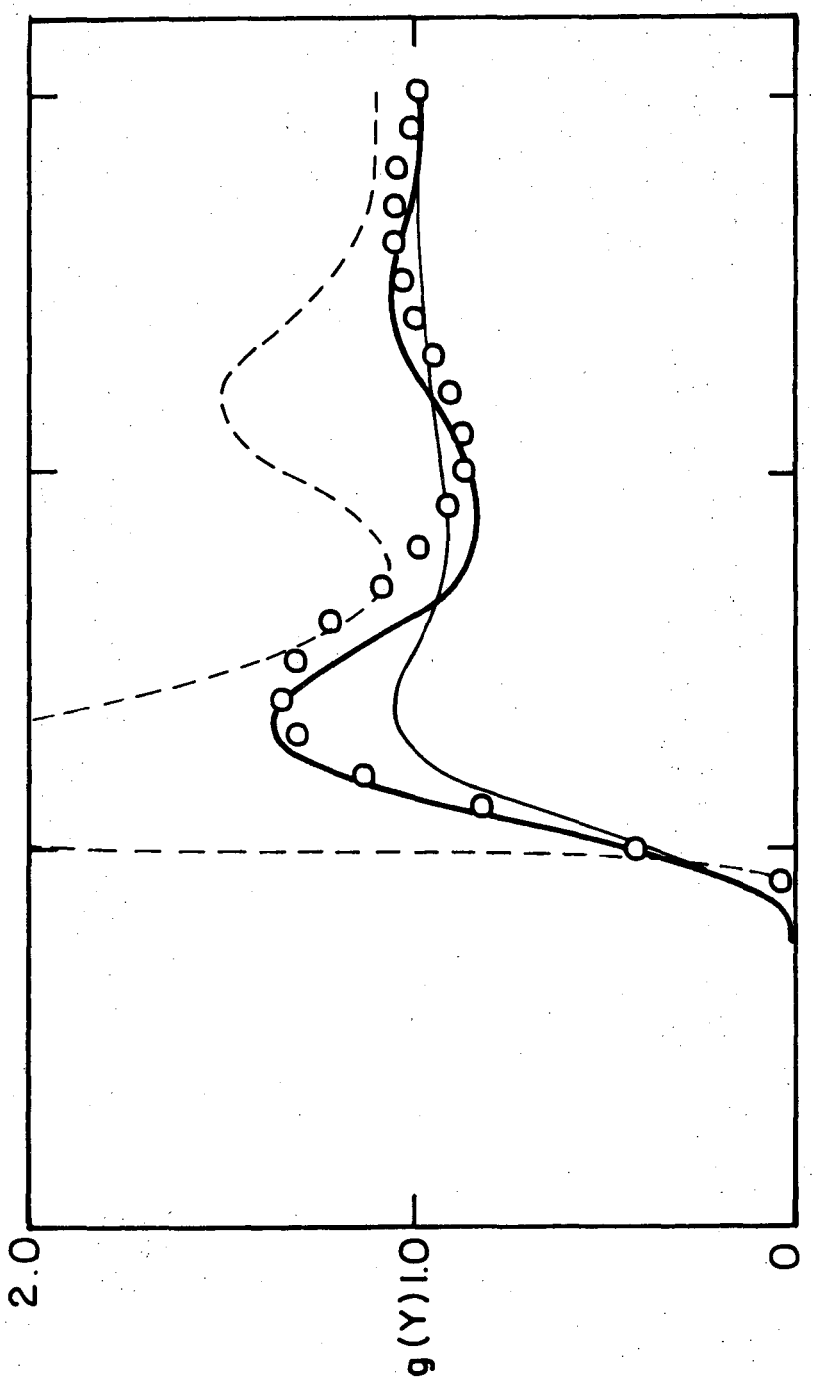

XBL 751-137

Fig. 1

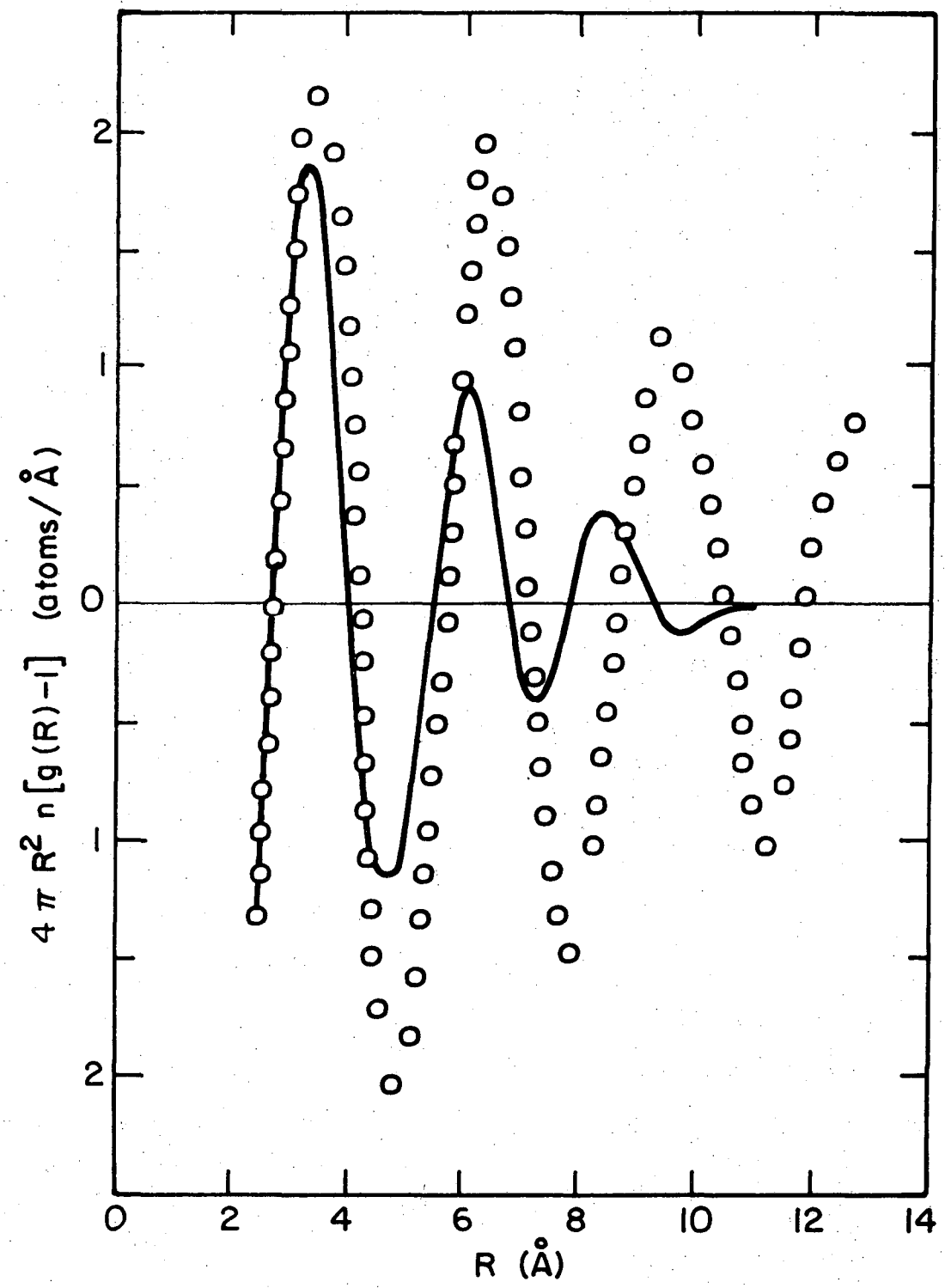

XBL 751-138

Fig. 2

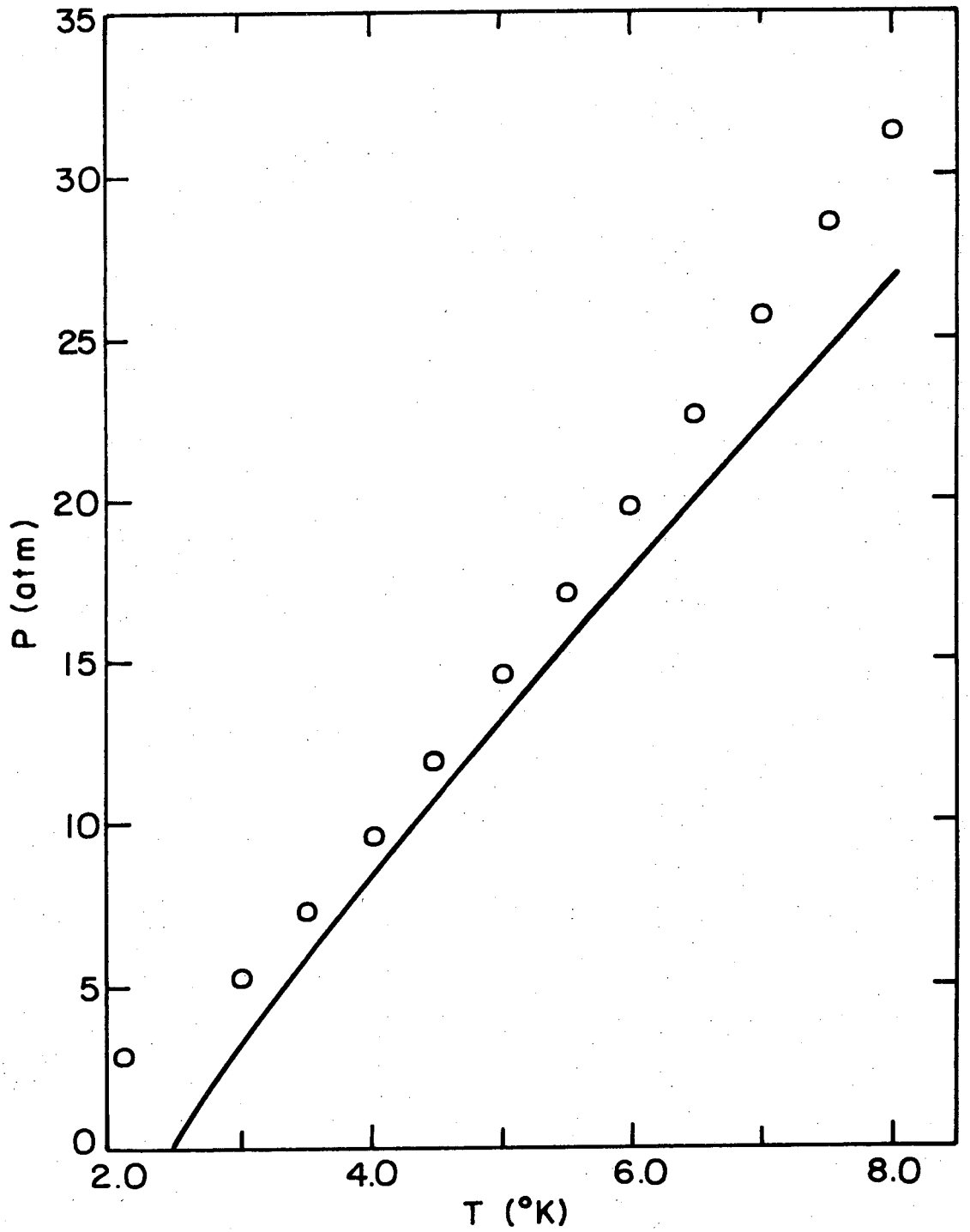

XBL 751-139

Fig. 3

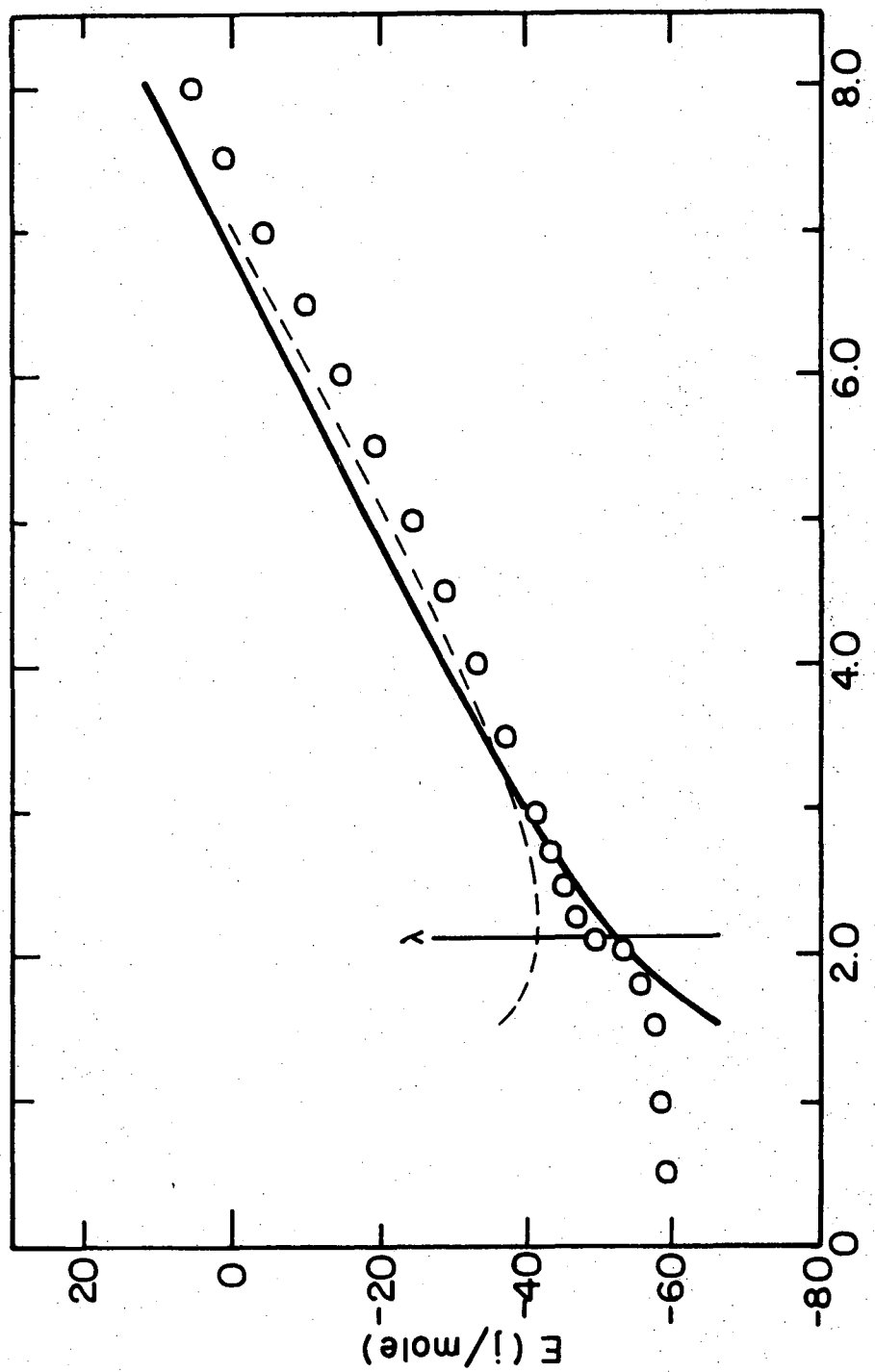

XBL 751-140

Fig. 4

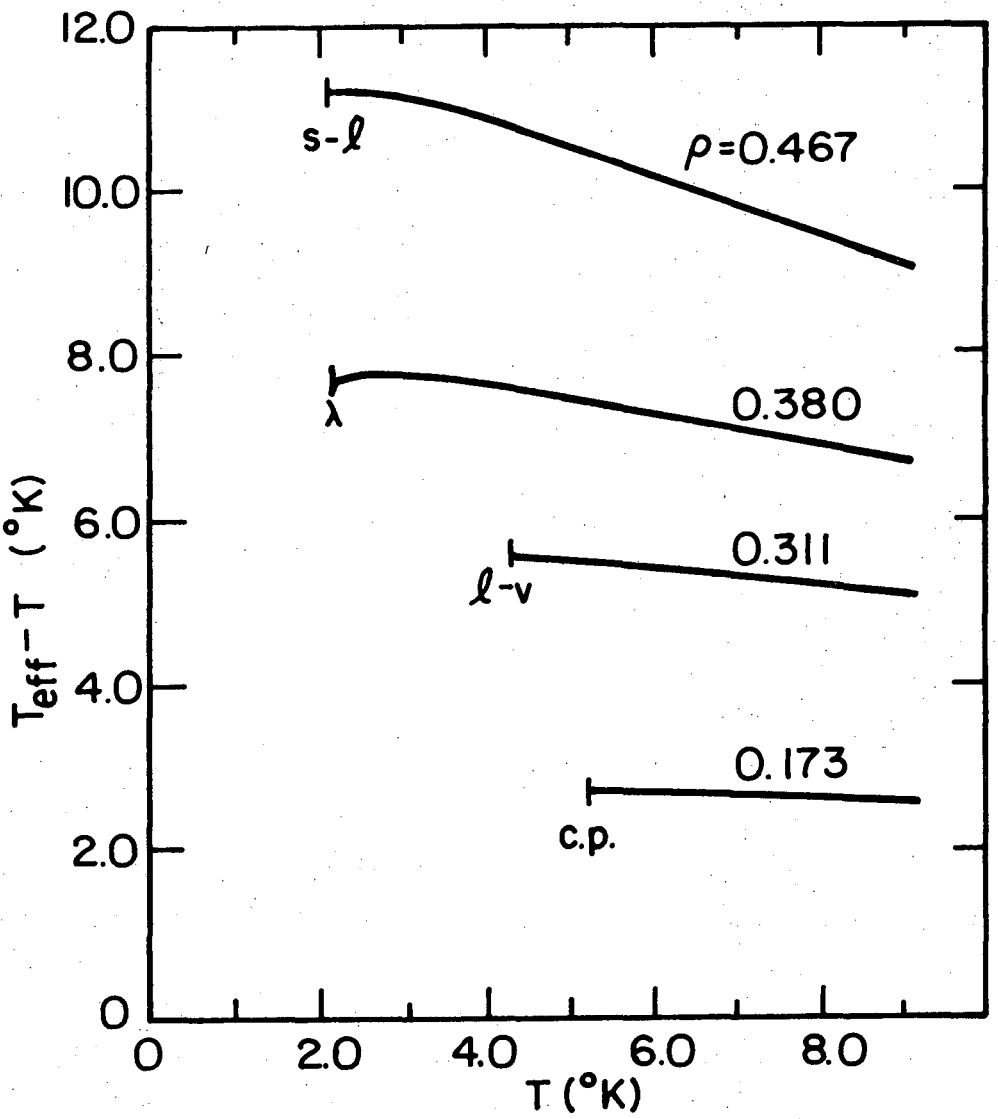
12.0
10.0
8.0
6.0
4.0
2.0
0
0
2.0
4.0
6.0
8.0
T (°K)
$T_{eff}-T$ (°K)
s-ℓ
ρ=0.467
λ
0.380
ℓ-v
0.311
c.p.
0.173
XBL 752-141

Fig. 5

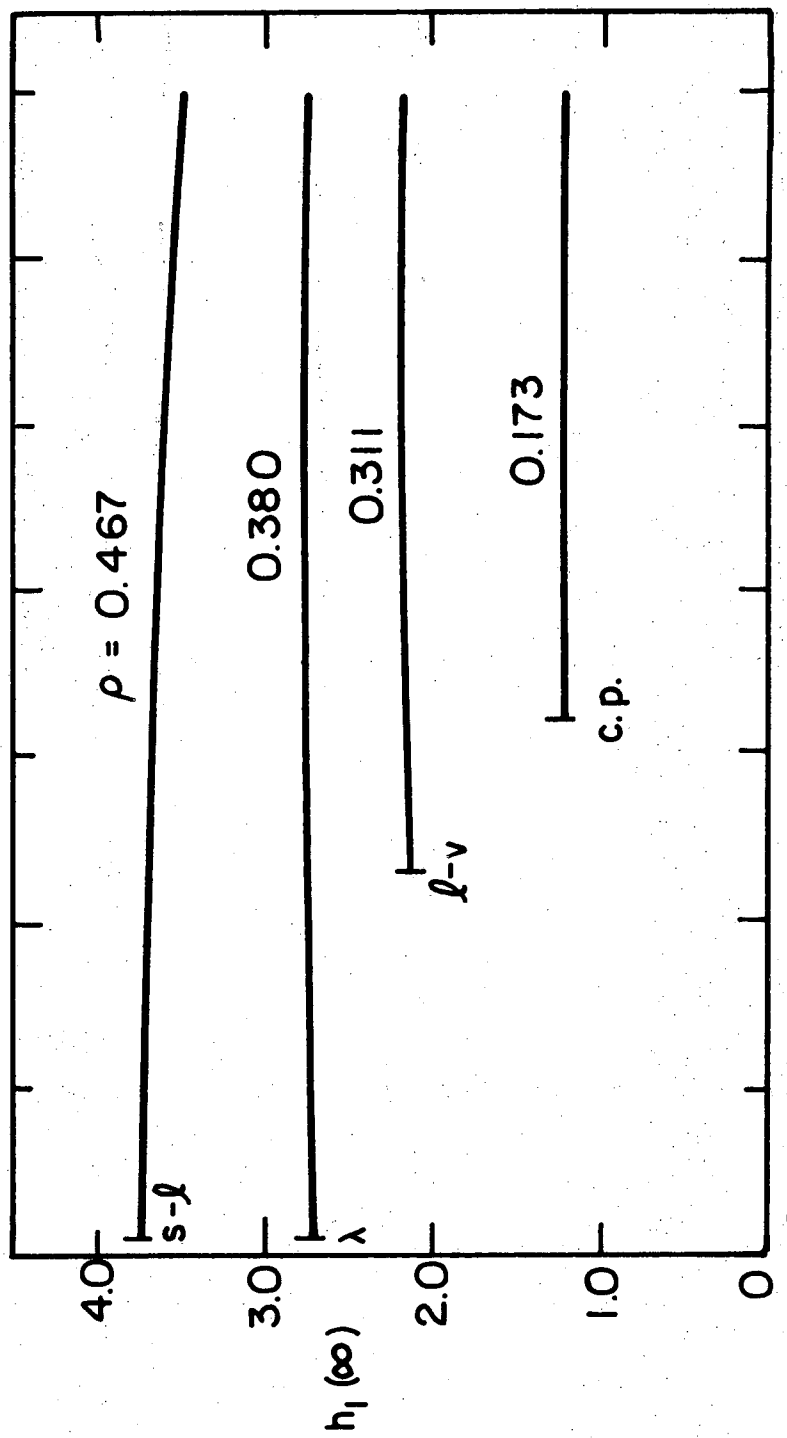

XBL 752-142

Fig. 6

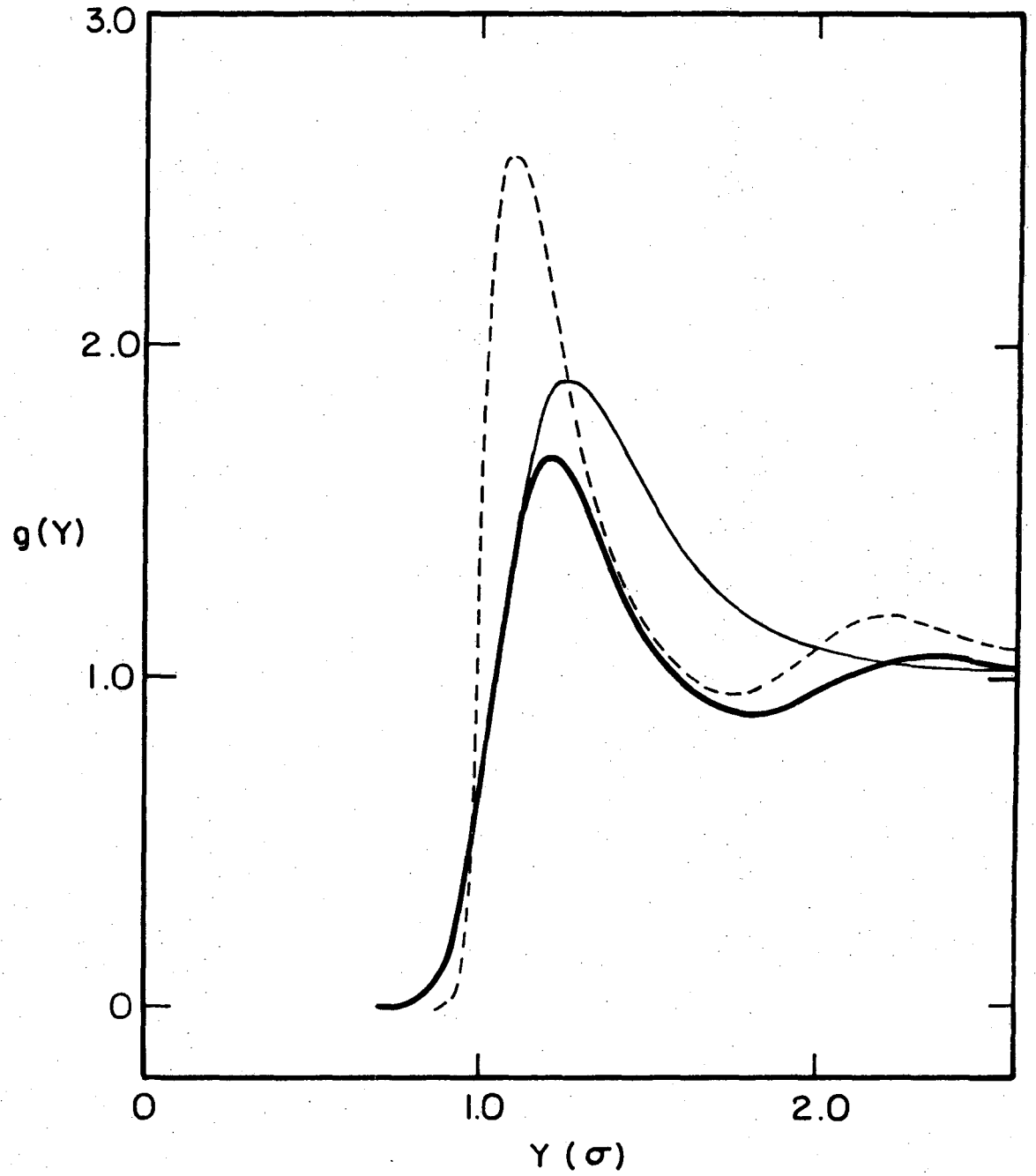

XBL 752-143

Fig. 7

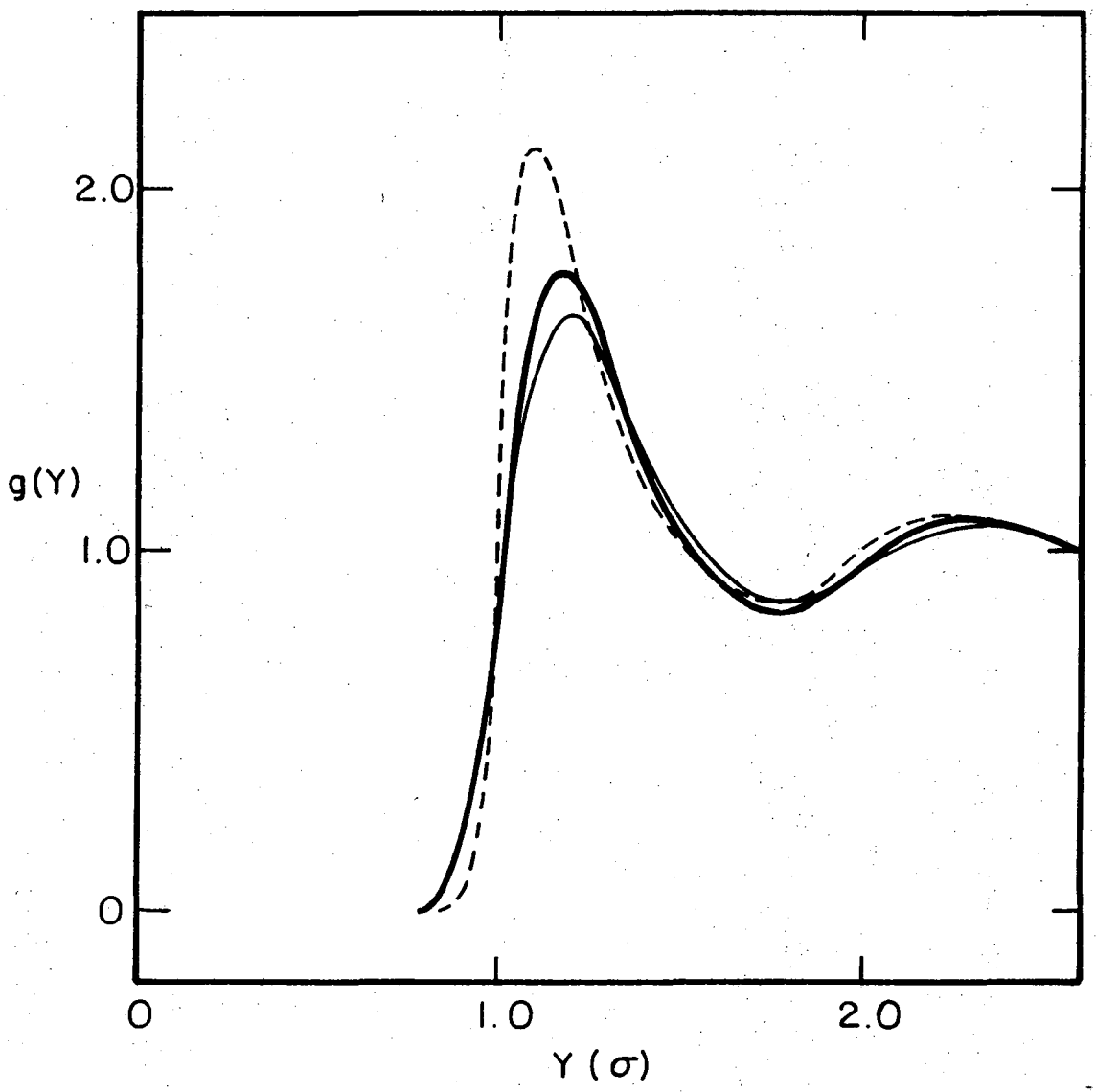

XBL 752-144

Fig. 8

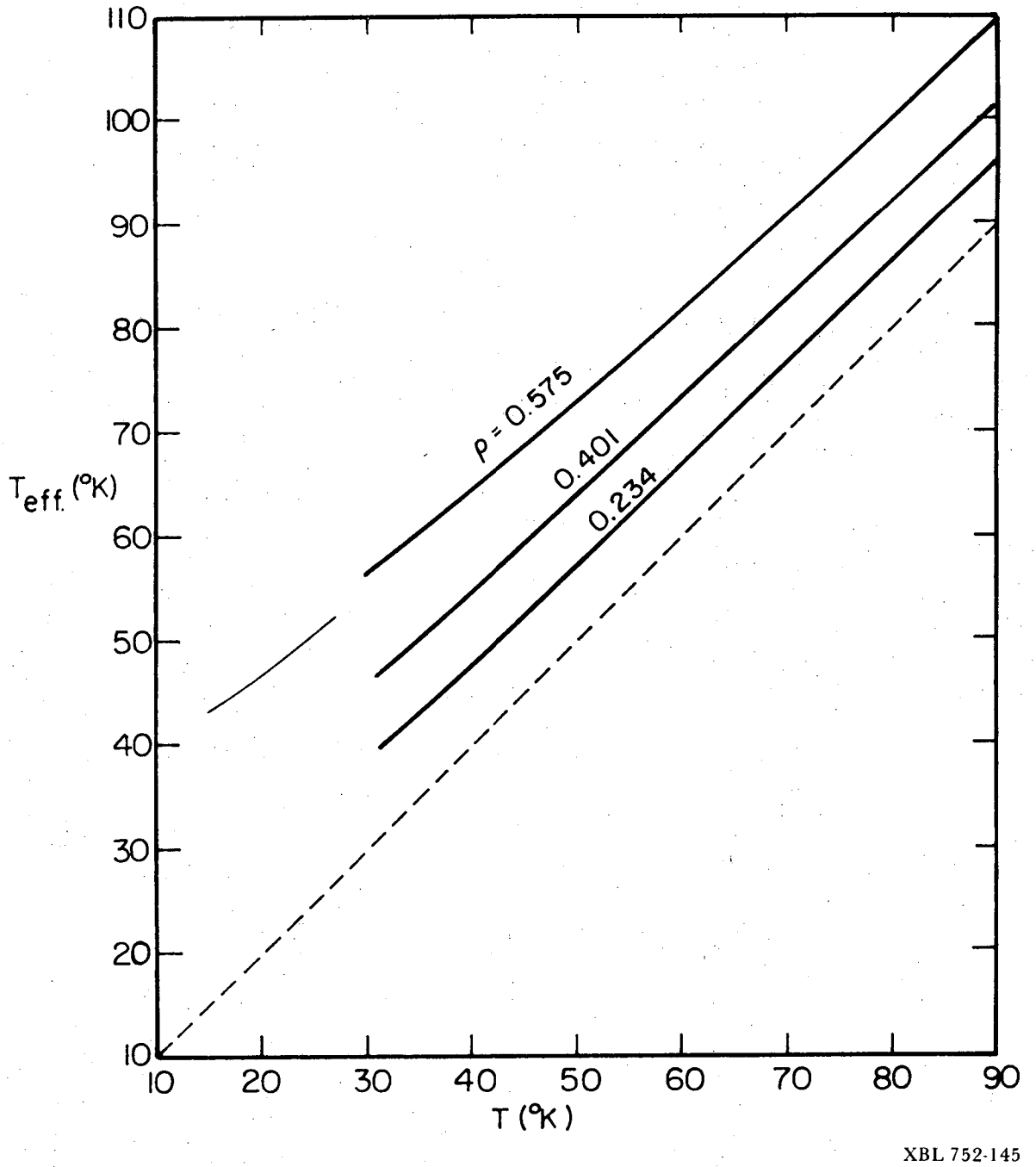
110
100
90
80
70
60
50
40
30
20
10
$T_{eff.}$ (°K)
ρ = 0.575
0.401
0.234
10
20
30
40
50
60
70
80
90
T (°K)
XBL 752-145

Fig. 9

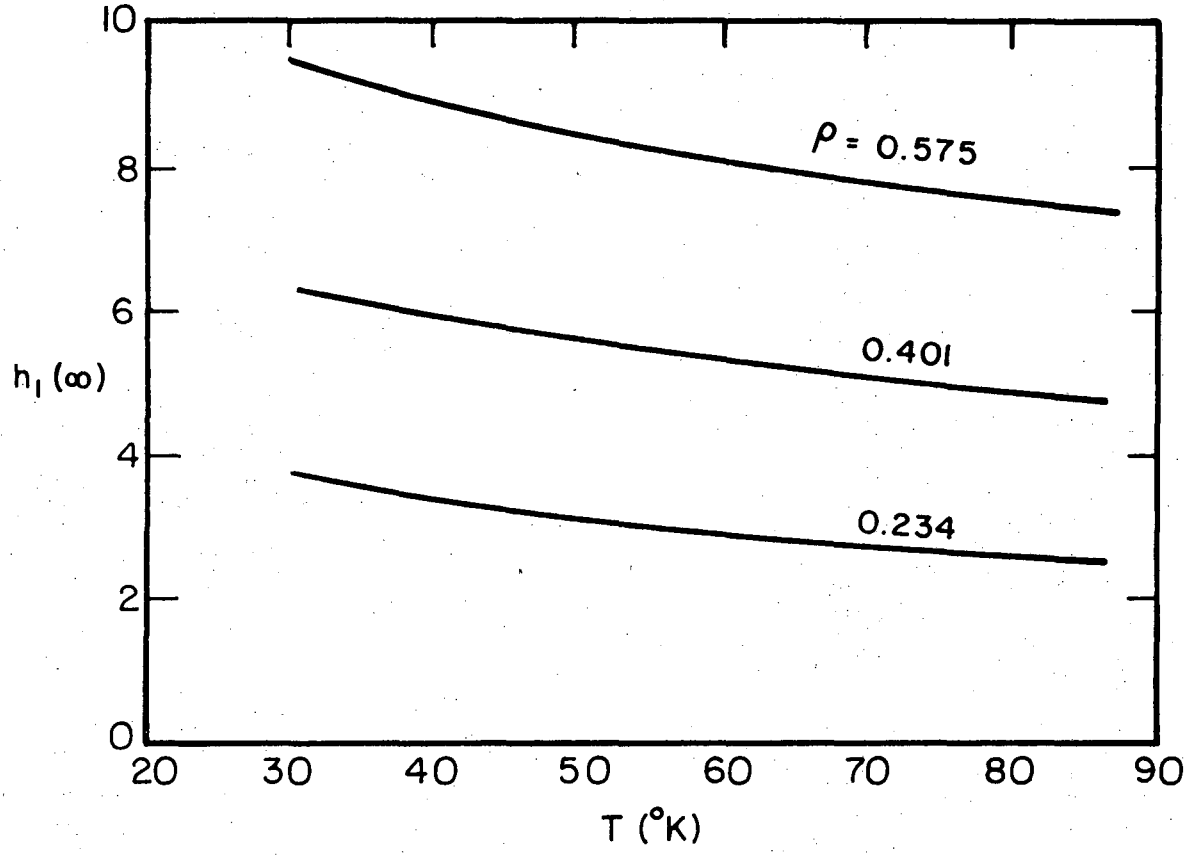

XBL 752-146

Fig. 10

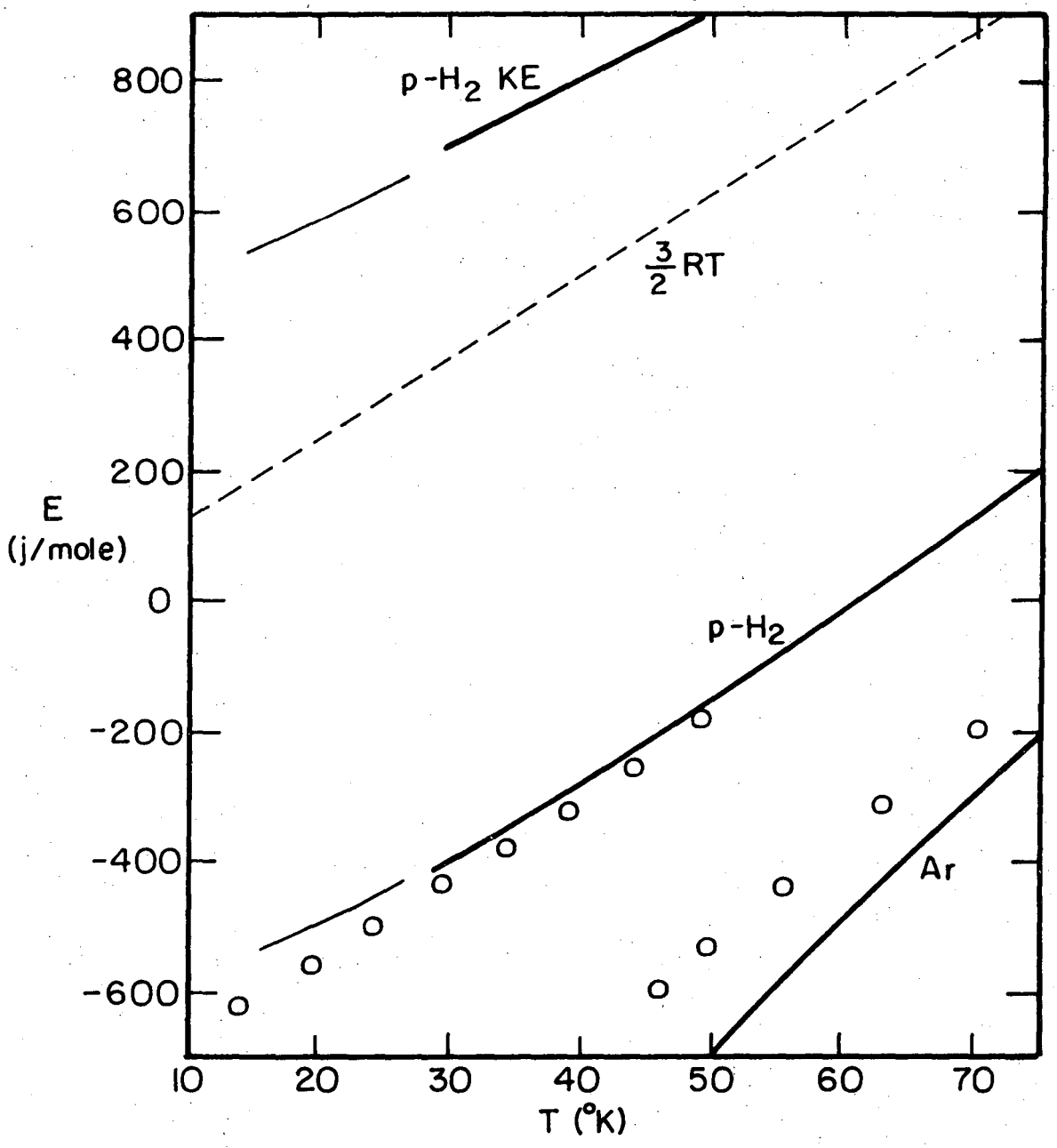

XBL 752-147

Fig. 11

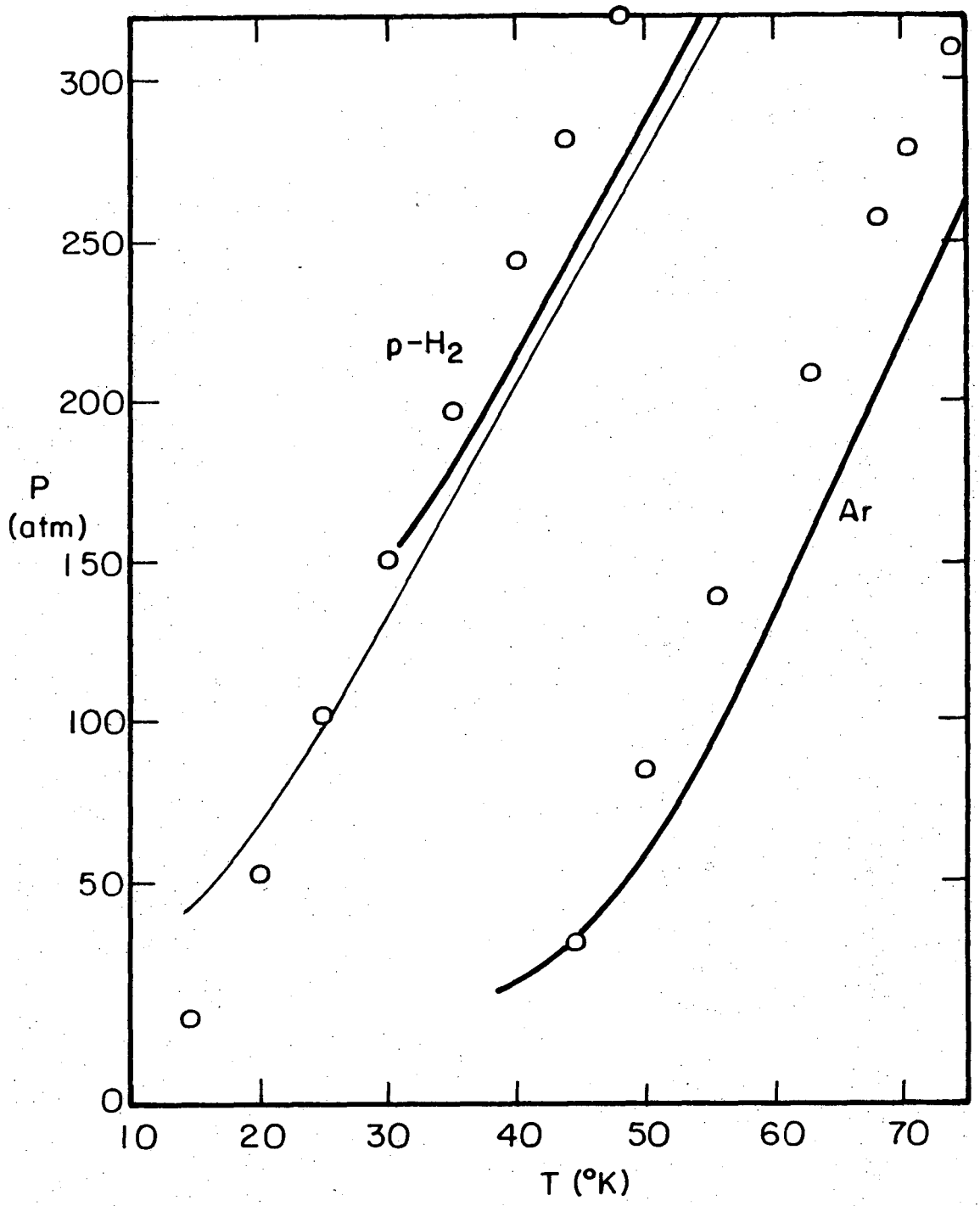

XBL 752-148

Fig. 12

TECHNICAL INFORMATION DIVISION
LAWRENCE BERKELEY LABORATORY
UNIVERSITY OF CALIFORNIA
BERKELEY, CALIFORNIA 94720